



Originally published as:

Tsukanov, N. V., Kramer, W., Skolotnev, S. G., Luchitskaya, M. V., Seifert, W. (2007): Ophiolites of the Eastern Peninsulas zone (Eastern Kamchatka): Age, composition, and geodynamic diversity. - *Island Arc*, 16, 3, 431-456

DOI: [10.1111/j.1440-1738.2007.00579.x](https://doi.org/10.1111/j.1440-1738.2007.00579.x).

Ophiolites of the Eastern Peninsulas zone (Eastern Kamchatka):

Age, composition, and geodynamic diversity

N. V. TSUKANOV¹, W. KRAMER², S. G. SKOLOTNEV,³ M. V. LUCHITSKAYA,³ AND W. SEIFERT²

¹*Institute of Oceanology, 117997, Nachimovskiy av. 36, Moscow, Russia,*
paleogeo@sio.rssi.ru phone: (095)1246563

²*GeoForschungsZentrum Potsdam, Telegrafenberg, D-14473 Potsdam, Germany,*
ws@gfz-potsdam.de phone: (0)331-2881375

³*Geological Institute Russian Academy of Sciences, 119017, Pyzhevskiy str, Moscow,*
Russia, luchitskaya@ginras.ru, skol@ginras.ru, phone: (095) 2308158

*Correspondence

Ophiolites of the Eastern Peninsulas zone (Eastern Kamchatka):

Age, composition, and geodynamic diversity

N. V. TSUKANOV,¹ W. KRAMER,² S. G. SKOLOTNEV,³ M. V. LUCHITSKAYA³ AND W. SEIFERT²

¹*Institute of oceanology, Moscow, Russia, paleogeo@sio.rssi.ru,*

²*GeoForschungsZentrum Potsdam, Germany, ws@gfz-potsdam.de*

²*Geological Institute Russian Academy of Sciences, 119017 Moscow, Russia (email:*

luchitskaya@ginras.ru, skol@ginras.ru,

Abstract

The geological, geochemical and mineralogical data of dismembered ophiolites of various ages and genesis occurring in accretionary piles of the Eastern Peninsulas of Kamchatka enables us to discriminate three ophiolite complexes: (1) Aptian–Cenomanian complex: a fragment of ancient oceanic crust, composed of tholeiite basalts, pelagic sediments, and gabbroic rocks, presently occurring in a single tectonic slices (Afrika Complex) and in olistoplaques in Pikezh complex of the Kamchatsky Mys Peninsula and probably in the mélangé of the Kronotsky Peninsula; (2) Upper Cretaceous complex, composed of highly depleted peridotite, gabbro, and plagiogranite, associated with island arc tholeiite, boninite, and high-alumina tholeiitic basalt of supra-subduction origin; and (3) Paleocene–Early Eocene complex of intra–island arc or backarc origin, composed of gabbros, dolerites (sheeted dikes) and basalts produced from oceanic tholeiite melts, and back arc basin (BAB)-like dolerites.

Formation of the various ophiolite complexes is related to the Kronotskaya intraoceanic volcanic arc evolution. The first ophiolite complex is a fragment of ancient Aptian–Cenomanian oceanic crust on which the Kronotskaya arc originated. Ophiolites of the supra-subduction zone affinity were formed as a result of repeated partial melting of peridotites in the mantle wedge up to the subduction zone. This is accompanied by

production of tholeiite basalts and boninites in the Kamchatsky Mys segment and plagioclase-bearing tholeiites in the Kronotsky segment of the Kronotskaya paleoarc. The ophiolite complex with intra-arc and MORB geochemical characteristics was formed in an extension regime during the last stage of Kronotskaya volcanic arc evolution.

Keywords: Ophiolites, paleoarc, geodynamic settings, mineral compositions, geochemistry, Eastern Kamchatka.

INTRODUCTION

Several allochthonous terranes, accreted to Asian margin in Cenozoic (Watson & Fujita 1985; Parfenov *et al.* 1993; Nokleberg *et al.* 1994; Geist *et al.* 1994; Sokolov & Byalobzhetskiy 1996; Konstantinovskaia 2001), govern the structure of the Eastern Kamchatka. The Kronotsky island arc terrane, extending in NE direction along Kamchatka Peninsula, is the most eastern one (Fig. 1). Its fragments outcrop in Eastern Kamchatka Peninsulas (Kamchatsky Mys, Kronotsky, and Shipunsky) (Bazhenov *et al.* 1992; Zinkevich *et al.* 1993). The structural piles of the Kamchatsky Mys and Kronotsky peninsulas, Eastern Kamchatka, display dismembered ophiolites of various ages and geneses. The Kronotsky volcanic arc existed in the form of a continuous island arc system starting from Late Cretaceous time: the oldest (Coniacian–Lower Campanian–Maastrichtian) island arc complexes are reported from the Kronotsky Peninsula (Raznitsyn *et al.* 1985); the volcanic activity terminated in Middle Eocene time (Zinkevich *et al.* 1993; Shcherbinina 1997; Boyarinoва *et al.* 2000; Levashova 2000). The Kronotsky paleoarc has been emplaced onto the Kamchatka continental margin between Upper Eocene to Early Miocene time (Zinkevich & Tsukanov 1993; Alexeiev *et al.* 1999; Alexeiev *et al.* 2006). Ophiolites are known only from the Kamchatsky Mys and Kronotsky peninsulas, whereas, in other parts of the island arc system, deposition was dominated by tuffaceous and volcanic or terrigenous and tuffaceous rocks. Currently, no consensus exists regarding the age, composition, or tectonic setting of the ophiolite fragments occurring in

the accretionary pile of the eastern peninsulas of Kamchatka (Nokleberg *et al.* 1994; Khotin 1976; Markovsky & Rotman 1981; Vysotsky 1989; Fedorchuk 1992; Osipenko & Anosov 2002). Some workers reassemble disintegrated fragments of peridotite, gabbro, and basalt from the Kamchatsky Mys Peninsula into a coherent ophiolite suite, interpreting these fragments to be derived from oceanic crust (Peyve 1987; Vysotsky 1989; Zinkevich *et al.* 1985). According to the data of Fedorchuk (1989), the Kamchatsky Mys ophiolite assemblage consists of at least three genetically different complexes, generated in contrasting geodynamic settings: oceanic basement, oceanic cover, and island arc. In some papers (Osipenko & Anosov 2002), Eastern Kamchatka ultramafic rocks are interpreted to comprise several NW-trending linear belts, each belt consisting of rocks with similar mineralogical and geochemical signatures. These belts are thought to have formed in “spatially stable deep-seated zones of magma generation” (Osipenko & Anosov 2002).

We have studied ophiolite associations of the Kamchatsky Mys and Kronotsky peninsulas (Fig. 1). The ophiolitic rocks occurring in different segments of the Kronotsky paleoarc can be reassembled into several ophiolite suites of different ages originating from complexes of different geodynamic settings (Kramer *et al.* 2001; Skolotnev *et al.* 2003). In addition, it will be shown that ophiolites from different segments of the Kronotsky paleoarc have different compositions, which suggests arc basement heterogeneity and diversity of geodynamic settings that produced ophiolites as the island arc kept evolving. This paper presents data and results from many years of our study and comprehensive geological analysis of the age and chemistry of a variety of ophiolite fragments found in Eastern Kamchatka.

GEOLOGICAL FRAMEWORK

The Kamchatsky Mys and Kronotsky peninsulas have composite fold-and-thrust architecture, incorporating volcanic, terrigenous and volcanoclastic (particular by tuffaceous) rocks of Cretaceous and Paleocene–Eocene ages and tectonic slices of serpentinite mélangé, gabbro, and ultramafic rocks (Khotin 1976; Zinkevich *et al.* 1985; Raznitsyn *et al.* 1985; Fedorchuk 1989; Shapiro *et al.* 1987; Zinkevich *et al.* 1993; Zinkevich & Tsukanov 1993; Boyarinova *et al.* 2000, 2001; Saveliev 2004).

In the structure of ***Kamchatsky Mys Peninsula*** two blocks are distinguished: northern – Stolbovskoy and southern – Afrika (Fig. 1a).

The Stolbovskoy block mainly consists of homoclinally occurring tuffaceous and volcanic complexes of the Stolbovskaya (Maastrichtian–Eocene) Group (Khotin 1976; Beniyamovsky *et al.* 1992; Boyarinova *et al.* 2000). Volcanic rocks predominate in the lower part of the section (Tarkhovskaya Formation); they consist of island arc tholeiites and boninites (Khubunaya 1987; Fedorchuk 1989).

The Afrika block has a composite fold-and-thrust structure of south and southwest vergence (Fig. 1a). The structural pile of the Kamchatsky Mys Peninsula incorporates several allochthonous complexes overlain by Miocene–Pliocene and Pliocene–Quaternary formations. They are composed of (i) effusive, siliceous and carbonate rocks of the Aptian–Cenomanian Afrika Complex, (ii) tuffaceous, siliceous and terrigenous rocks of the Campanian–Maastrichtian Pikezh Complex, (iii) basaltic lavas and volcanoclastic and terrigenous sediments of the Paleocene–Early Eocene Kamensk Complex, (iv) serpentinite mélangé, (v) spinel peridotite and serpentinitized peridotite from the Mt. Soldatskaya Massif, and (vi) gabbro, gabbro-dolerite and dolerite of the Olenegorsk Pluton (Zinkevich *et al.* 1985; Fedorchuk 1989; Khotin 1976; Skolotnev *et al.* 2001; Tsukanov & Fedorchuk 2001). Rocks of the Olenegorsk Pluton form the lower structural unit in this thrust package. They are overthrust by a package of tectonic slices composed of Paleocene–Early Eocene (Kamensk complex), Campanian–Maastrichtian formations

(Pikezh complex) and serpentinite mélangé and peridotites of Mt. Soldatskaya Massif (Khotin 1976; Vysotsky 1989; Fedorchuk 1989). According to the data of Fedorchuk (1989) and Saveliev (2004) there are alkaline basalts in the field of Pikezh complex development. Their interrelationship with the host rocks of Pikezh complex is not clear. Saveliev (2004) considers the alkaline basalts as thin lava-flows. We suppose that these basalts may form thin tectonic slices in tuffs of the Pikezh complex.

Aptian–Cenomanian rocks (Afrika Complex) commonly occur in the form of thin tectonic slices and large olistolithes among Upper Cretaceous deposits (Pikezh complex) or in serpentinite mélangé.

Ophiolite fragments of the Kamchatsky Mys Peninsula (Fig. 1a) consist of (i) gabbroic rocks and dolerites of the Olenegorsk Pluton, (ii) ultramafic rocks of Mt. Soldatskaya Massif, (iii) gabbro blocks with plagiogranite in serpentinite mélangé, (iv) basalts and calcareous rocks, jasper, and cherts of the Aptian–Cenomanian Afrika Complex, and (v) basalts and mudstones of the Paleocene– Early Eocene Kamensk Complex.

The ***Kronotsky Peninsula*** displays Coniac-Campanian-Maastrichtian rock complexes of the Kamenistskaya and Eocene Kronotskaya Formations, consisting of pillow-basalt alternating with hyaloclastite, tuff, tuffite, siliceous, and tuffaceous conglomerate (Raznitsyn *et al.* 1985; Shcherbinina 2000; Boyarinova 2001) (Fig. 1b). Structurally, the eastern part of the peninsula forms a large anticlinal fold with thrusting limbs. Paleogene deposits make up a monocline pile. Basalts of Kamenistskaya and Kronotskaya Formations, according to Khubunaya (1987), are classified as plagioclase-bearing tholeiites. A tectonic slice of serpentinite mélangé separates tuffaceous and volcanic island arc complexes of the Kamenistskaya (Upper Cretaceous) and Kronotskaya (Eocene) Formations. Pebbles of serpentinitized peridotite are found in tuffaceous conglomerates of the Kronotskaya Formation (Raznitsyn *et al.* 1985).

Ophiolites of the Kronotsky peninsula consist of peridotite, gabbro, dolerite, basalt, amphibolite, plagiogranite, rodingite, and opicalcite blocks in serpentinite mélange. Here, a large massif of serpentized harzburgite with lenticular dunite bodies 300 m in thickness and covering an area of 12 km² was mapped (Raznitsyn *et al.* 1985; Boyarinova 2001; Skolotnev *et al.* 2003) (Fig. 1b).

In the Shipunsky segment of the Kronotskaya paleoarc, no ophiolitic rocks crop out. In the Shipunsky Peninsula, Maastrichtian(?)–Middle Eocene volcanic and tuffaceous complexes are widespread (Tsukanov *et al.* 1991).

FIELD RELATIONS

Ophiolites of the Kamchatsky Mys Peninsula were studied from the Olenegorsk Pluton and Mt. Soldatskaya Massif and from near the sources of the Pervaya Olkhovaya and Pervaya Perevalnaya rivers (Fig. 1a).

The structure of the Mt. Soldatskaya peridotite massif was studied in outcrops along the Belaya River. The lower part of the massif is composed of fresh medium-grained peridotite (200 m thick), cut by numerous faults. Serpentinized peridotites crop out in the middle part of the massif (nearly 100 m thick). The serpentinite mélange occupies the upper structural position. It extends further to the north-east to the 1st Olkhovaya River. The mélange contains large blocks of pillow-basalt, amphibolite, amphibole schist, greenschist, tuff, chert, gabbro, basalts and thin-layered pelagic sediments of Aptian-Albian and Albian – Senomanian age (Fedorchuk 1989; Zinkevich *et al.* 1993).

The structure and composition of the Olenegorsk Pluton were studied in outcrops along the Olenya, Stremitelnaya, Vodopadnaya Rivers, and Kamenny Stream (Fig. 2).

Olenegorsk Pluton is made up of several tectonic slices, composed of gabbroic rocks with dolerite dikes (Fig. 2). Gabbroic rocks are mainly represented by diallage gabbros with rare coarse-grained olivine gabbro-norite schlieren of 1.5-3 m thickness (Kamenny Stream). The dolerite dikes, which are 0.5–5 m in thickness, cross-cut the gabbro. In some places we observe numerous roughly parallel nearly vertical dikes resembling a sheeted

dike complex (Vodopadnaya and Stremitelnaya Rivers). Along the contacts of the tectonic slices, serpentinite mélangé is developed. The mélangé contains blocks of gabbro, dolerites and rodingite. Near these contacts the gabbro section shows numerous serpentinite enclaves (0.1–5 m size) (Fig. 3a-e). The nearly 10 m wide outcrops of a layered series are likely related to the same zone of serpentinite mélangé (Vodopadnaya and Stremitelnaya Rivers).

The Olenegorsk Pluton is tectonically overlain by a strongly tectonized pillow-basalt with thin interlayers of jasper and cherty mudstone Paleocene–Early Eocene age (Vysotsky 1989) (Kamensk complex) (Fig. 2). The latter is overthrust by Upper Cretaceous Pikezh complex (Fedorchuk 1989). It hosts olistoliths of limestone, jasper, and pillow basalt of Albian–Cenomanian age (Fedorchuk 1989).

In the west and northwest of the source region of the Pervaya Olkhovaya and Pervaya Perevalnaya rivers, serpentinite mélangé is widespread. It contains blocks of pillow-basalt, amphibolite, amphibole schist, greenschist, tuff, chert, and gabbro. A large gabbro body, 1.5 km across and not less than 100 m thick, was studied there (Fig. 4). The gabbro contains plagiogranite making a network of veins of irregular shape 1 to 5–7 cm thick and dike-like bodies about 1.5–2.0 m thick, which intrude the gabbro and contain angular gabbroic xenoliths (Fig. 3f). Besides, here one finds plagiogranite porphyry dikes which are 5–7 m in thickness, cutting the gabbro and dolerite dikes (Tsukanov *et al.* 2004).

Southeast of the region, one finds a broad syncline consisting of predominantly tuffaceous and terrigenous deposits of Late Cretaceous age (Pikezh Complex). At the Pervaya Perevalnaya River, there are blocks of pillow-basalts, in places associated with jasper and pink limestone, which are not stratified but consist of small (5–10 m) irregular blocks occurring in the tuffs of the Pikezh Complex.

On the Kronotsky Peninsula, ophiolitic rocks were studied in its eastern part: along the Neudobny Creek, the Buy Creek, along the Bolshaya River and Cape Kronotsky (Fig. 1b).

In this area, one may see massive peridotites and serpentinite melange with peridotite, gabbroic rock, basalt, dolerite and amphibolite blocks.

PETROGRAPHY

OPHIOLITES OF THE SOUTHERN KAMCHATSKY MYS PENINSULA

Mt. Soldatskaya Massif. Ultramafic rocks from the lower part of the Mt. Soldatskaya Massif are classified as clinopyroxene-bearing harzburgites. Clinopyroxene grains account for not more than 5% by volume. The peridotites have protogranular texture consisting of pyroxene and olivine, in which grains of brown spinel form mostly xenomorphic sometimes subhedral or vermicular inclusions. Often the spinels are intergranular filling. Up the sequence, fresh rocks give way to serpentinite, in which some spinel and clinopyroxene grains are preserved whereas olivine and orthopyroxene occur only in the form of relict grains surrounded by serpentine.

Olenegorsk Pluton. We studied the rocks of the layered series in two small tectonic blocks, enclosed in gabbro in the Olenegorsk Pluton. On the right bank of the Stremitelnaya River, the structure of this block is extremely heterogeneous due to irregular distribution of the major constituents olivine, plagioclase, and pyroxenes. On the right bank of the Vodopadnaya River, a small block in serpentinite mélangé contains lenses and layers (5–20 cm thick) of anorthosite in massive serpentinite. Some of these lenses are surrounded by haloes of small plagioclase segregations. The serpentinite contains schlieren of plagioclase peridotite and troctolite (0.1–1 m across) and sections of rhythmic texture, in which thin (2–7 cm) layers of anorthosite and troctolite alternate. This rhythmicity is not uniform.

Depending on the proportions of the major constituents in different localities through the body, the rocks may be classified as anorthosite, serpentinite after peridotites and plagioclase-bearing peridotite, as troctolite, pyroxene-bearing troctolite, and olivine gabbro-norite. In the pyroxene-bearing troctolite, among olivine aggregates occur xenomorphic segregations of irregular shape (0.2–1 cm across) composed of pyroxene

(mainly clinopyroxene) and plagioclase grains. In the troctolite those segregations are composed of plagioclase with sporadic clinopyroxene grains.

The gabbroic rocks of the Olenegorsk Pluton are dominated by gabbro *sensu stricto* with gabbroic texture, in places containing small amounts of orthopyroxene. The accessory minerals are magnetite and, less frequently, ilmenite. Secondary alterations are, as a rule, insignificant. The clinopyroxene is, in places, partly altered to amphibole (actinolitic hornblende); and the plagioclase may be replaced by hydrogrossular, prehnite and chlorite. In many previous papers, these rocks were referred to as “diabase gabbro.”

Olivine gabbro-norite occurs in schlieren in the diabase gabbro. One of the schlierens, nearly 2 m across, was studied in the lower reaches of the Kamenny Stream. Partly the olivine gabbro differs from the typical gabbro in containing xenomorphic segregations of irregular shape, each composed of several small olivine grains, stretching in chains. The olivine is partly or completely replaced by serpentine, smectite and chlorite.

The Olenegorsk Pluton gabbros contain numerous serpentinite enclaves. Around the enclaves, the gabbro texture changes sharply, becoming very coarse grained. As a rule, at the contact with the serpentinite, the plagioclase in the gabbro is replaced by prehnite, and the clinopyroxene shows strong plastic deformation.

Olkhovaya Gabbro Block. The gabbroic rocks comprise fine-grained hornblende gabbro and gabbro-norite and are intruded by plagiogranite dikes. They show strong secondary alteration (low-grade metamorphism). The clinopyroxene is partly or completely replaced by a variety of amphiboles, and prehnite was formed within plagioclase.

The plagiogranites are fine-to medium-grained and have equigranular texture; less frequently, they have granophyric texture composed of vermicular intergrowths of quartz and plagioclase. The plagiogranites are mainly composed of plagioclase and quartz. The mafic minerals are biotite and amphibole (< 5%); the accessory minerals are zircon, apatite, sphene, and an ore mineral; and the alteration assemblage includes chlorite, epidote, zoisite, sericite and saussurite.

Volcanic and subvolcanic rocks. The dolerites, occurring as dikes, have fine- to medium-grained ophitic to plagiophyric ophitic texture and are mainly composed of plagioclase and clinopyroxene with some titanomagnetite (3–5%). The clinopyroxene is often partly or completely replaced by chlorite and actinolite; medium- to low-Na plagioclase by albite (domains and rims), epidote, and sericite; and titanomagnetite by sphene and leucosene. The basalts of Afrika and Kamensk complexes are intersertal, aphyric to weakly porphyritic, by plagioclase, clinopyroxene and olivine phenocrysts. They are often hyaline (particularly pillow lavas and pyroclastic fragments) and may be slightly porous. The groundmass is composed of plagioclase microlites (often with swallow tails and other forms of skeletons), clinopyroxene, glass and ore mineral (3–5%). Alteration minerals, which replace primary minerals and form fill in vesicles are glauconite, smectite, chlorite, Fe-hydroxides and albite. Alkaline basalts occur occasionally. They have trachydoleritic and doleritic texture and are composed of plagioclase laths, clinopyroxene, potassic feldspar, minor amphibole, biotite, and ore minerals (Saveliev, 2004).

OPHIOLITES OF THE EASTERN KRONOTSKY PENINSULA

The peridotites, according to their mineral composition (nearly 5% clinopyroxene), may be classified as clinopyroxene-bearing harzburgite. The olivine is extensively replaced by serpentine (90–95%), but unaltered relict grains are also preserved. The gabbro-pegmatites are gabbro-norites with orthopyroxene prevailing over clinopyroxene. The rocks are in places recrystallized to a granoblastic aggregate with irregular titanomagnetite segregations in the intergranular space. Mafic minerals are extensively replaced by actinolite. The pyroxenites together with the gabbro-pegmatites form veins and dikes. They have medium-grained euhedral granular texture and are composed of clinopyroxene and orthopyroxene. Very coarse-grained gabbro, gabbro-diabase, olivine augen-gabbro and amphibolite are observed making blocks ranging in size from 1 to 30 m across in serpentinite mélangé. The gabbro-diabase and very coarse-grained gabbro are composed

of clinopyroxene, partly replaced by actinolite and chlorite, and plagioclase, partly albitized. An ore mineral occurs sporadically. The olivine augen-gabbro has porphyroclastic texture. Sporadic porphyroclasts of clinopyroxene are located among clinopyroxene neoblasts and among (prevailing) olivine neoblasts. The secondary minerals are chlorite, prehnite, and hydrogrossular. The amphibolites have thin-layered structure and granoblastic texture. They consist of alternating layers composed of hornblende and oligoclase-andesine. Rare relics of clinopyroxene are preserved; ilmenite, titanomagnetite, and magnetite grains are observed besides.

ANALYTICAL METHODS

The main data set for ultramafic to mafic rocks were analyzed in the geochemical laboratory of the GeoForschungsZentrum Potsdam. Major elements, Cr, Ni, V, Zn, and partly Ba, Rb, Sr, and Zr were analyzed by X-ray fluorescence. FeO has been determined by means of potentiometric titration following oxidizing decomposition. After catalytic combustion the H₂O and CO₂ were determined coulometrically. Rare earth element (REE), Y and Sc abundances were analyzed by Inductively Coupled Plasma – Optical Emission Spectrometry (ICP-OES) after sample fusion with sodium peroxide, chromatographic separation and concentration following the methods of Zuleger & Erzinger (1988). The abundances of Cs, Hf, Nb, Ta, Th, U and low contents of Rb, Sr and Zr were determined by Inductively Coupled Plasma – Mass Spectrometry (ICP-MS). The analytical accuracy of the trace element determinations is better than 10%. The major constituents of normal-mid-oceanic ridge basalt (N-MORB)-type volcanic rocks from the Kronotsky Peninsula were analyzed in the Kamchatskaya Searching Mapping Expedition, Petropavlovsk-Kamchatsky, Russia. The major elements of felsic rocks were analysed at the Analytical Center of the Geological Institute of the Russian Academy of Sciences, Moscow, Russia. Trace elements including REE in felsic rocks were analyzed by ICP-MS at the Institute of Mineralogy and Geochemistry of Trace Elements, Moscow, Russia (analyst: D.Z. Zhuravlev). Mineral compositions from ultramafic and mafic rocks were

measured on a Cameca SX100 electron microprobe in the geochemical laboratory of the GeoForschungsZentrum Potsdam.

WHOLE ROCK CHEMISTRY

Tables 1 to 3 show a wide selection from the major and trace element data of the ophiolite members of the southern Kamchatsky Mys and eastern Kronotsky Peninsulas. We analyze mainly REE and trace element contents because they are the most informative elements concerning rock genesis.

OPHIOLITES OF THE SOUTHERN KAMCHATSKY MYS PENINSULA

Mt. Soldatskaya Massif. The major element chemistry of the spinel peridotites from the Mt. Soldatskaya Massif (contents SiO_2 , MgO and FeO^*) (Table 1) shows a perceptible variability, which seems to be correlated to the degree of serpentinitization and expressed by the H_2O content, but Mg# is nearly constant (see Table 1). The rocks are depleted in Ti, Al and Ca ($\text{TiO}_2 = 0.005\text{-}0.008\%$, $\text{Al}_2\text{O}_3 = 0.1\text{-}0.6\%$, $\text{CaO} = 0.10\text{-}0.85\%$). The spinel peridotites have increased LREE: $(\text{La}/\text{Eu})_n = 1.86$, show low MREE contents of 0.04 to 0.10 ppm and low HREE contents from Dy to Er (Fig. 5a), have MREE depletion relative to HREE: $(\text{Lu}/\text{Eu})_n = 6.3$ (Fig. 5a). Therefore, they are similar to SSZ peridotites like the Troodos ultramafics according to Kay and Senechal (1976).

Olenegorsk Pluton. Diabase gabbros from the Olenegorsk Pluton are lower in titanium, sodium, potassium, and phosphorus ($0.17\text{-}0.38\%$ TiO_2 , $1.57\text{-}2.21\%$ Na_2O , $0.01\text{-}0.04\%$ K_2O , $<0.01\text{-}0.02\%$ P_2O_5) and distinctly higher in magnesium and calcium ($9.0\text{-}10.4\%$ MgO , $12.0\text{-}14.2\%$ CaO) compared to the basalts (Table 1). In the olivine gabbro-norites, SiO_2 and TiO_2 contents are lower and MgO contents are higher than in the diabase gabbros. The REE patterns in the diabase gabbros are similar to those in the cumulates crystallized from N-MORB melts: $(\text{La}/\text{Sm})_n = 0.3\text{-}0.9$, $\text{La}_n = 1.5\text{-}2.8$, $\text{Sm}_n = 3\text{-}4.5$, $\text{Lu}_n = 2.8\text{-}6$; distinct positive Eu-anomaly is noted (Fig. 5b). Major- and trace element contents of parts of the Olenegorsk Pluton represent ultramafic members of the layered rock series rocks (see the plagioclase peridotites 9814-4 and 9814-10 in Table 1). These bear SiO_2 contents like

spinel peridotites but have MgO values ranging between gabbroic rocks and spinel lherzolites. Their REE patterns are similar to those of the gabbros, but REE totals are lower than in the gabbros.

Some of enclaves within gabbroic rocks have, apart from LREE, chemical composition similar to the plagioclase peridotite from the Olenegorsk Pluton (compare sample 9814-10 and 0243/1 in Table 1). Other enclaves (cf. 0225/2 and 0230/1) are serpentinized, less depleted peridotites. Their Mg# are smaller and their TiO₂, Zr and REE values are 3 to 10-times as high as in Mt. Soldatskaya spinel peridotite. The enclaves form distinct curves separated from the Mt. Soldatskaya and Kronotsky peridotites in the REE distribution diagram (Fig. 5a).

Olkhovaya Gabbro Block. In terms of bulk rock chemistry, gabbroic rocks from the source of the Pervaya Olkhovaya River are similar to those of the Olenegorsk Pluton (Table 1). Their REE totals are nearly 1–4 times the chondrite value. The REE patterns in the gabbroic rocks are nearly flat and similar to those of N-MORBs; i.e., the plots dip down from MREE to LREE (Fig. 6a). The relatively low TiO₂, Y, and Zr contents (0.16-0.91%, 4.3-13 ppm, and 5-46 ppm, respectively) render them similar to the Philippine Sea gabbroic rocks (Fig. 7a).

The SiO₂ vs. K₂O covariations indicate that plagiogranites are low-K rocks (Fig. 8). They are also low-Al granitoids (11.3–13.4% Al₂O₃, Table 1). The ocean ridge gabbro (ORG)-normalized (Pearce *et al.* 1984) patterns of the plagiogranites show low large-ion lithophile element (LILE) contents, approximately at the hypothetical ORG level, and high-field strength elements (HFSE) depletion; distinct Ta, and Nb minima are noted (Fig. 9). The plagiogranites show chondrite-normalized REE patterns with low, nearly 10-times chondritic value, REE totals, which are slightly higher than in the gabbroic rocks. Some of the patterns show REE contents similar to the gabbroic rocks, and positive Eu-anomaly (samples M11/6, M12/6); others are slightly LREE enriched and have weak negative Eu-anomaly (samples M-16, M12/3) (Fig. 6a).

Volcanic and subvolcanic rocks. Basalts of the Afrika and Kamensk complexes in terms of major and trace element chemistry are similar to each other in terms of moderately differentiated oceanic tholeiites: 1.25-1.99% TiO₂, 2.32-3.5% Na₂O, 0.68-2.02% K₂O, 0.12-0.23% P₂O₅, 5.69-7.16% MgO, and 8.39-10.6% CaO (Table 2). The REE totals are 20–50 times the chondritic value. The REE patterns of all basalt types mostly display weak Eu-anomalies. From their REE patterns ((La/Sm)_n = 0.4–0.7) (Fig. 5d) and from a comparison with N-MORB averages according to Sun & McDonough (1989) (Fig. 10c), most of these basalts are derived from depleted N-MORB melts. Some basalts from the Kamensk Complex have significantly higher potassium contents up to 2.0% K₂O (see samples 9801/1 and 9808/2, Table 2). In this case the La/Sm ratio is increased (0.9–1.0) indicating their derivation from less depleted T-MORB melts. However, the alkalis and other LILE may be higher because of their alteration, low-grade metamorphism included (smectitization, chloritization and sericitization) (Fig.10a to 10c).

Dolerites forming the dikes from the Olenegorsk Pluton are compositionally similar to the basalts just mentioned, differing from them in having lower potassium (0.04–0.26% K₂O) and sodium contents (1.90–2.45% Na₂O) and higher magnesium (8.0–8.9% MgO) (Table 1). The REE patterns of the dolerites are roughly parallel to N-MORB (compare diagrams of Fig. 5d), but their REE totals are lower (15–20 times the chondritic value; (La/Sm)_n = 0.4–0.6; weak negative Eu-anomalies are observed.

OPHIOLITES OF THE EASTERN KRONOTSKY PENINSULA

Chemically, serpentized harzburgites differ from Mt. Soldatskaya rocks in having higher contents of titanium, aluminum and calcium (0.01-0.02% TiO₂, 0.70-1.3% Al₂O₃, 0.10-1.45% CaO) and lower magnesium (37.7-38.6% MgO), the latter mainly due to the generally high degree of serpentization (Table 3). The REE from La to Gd are similar in the peridotites of both areas, but the more stable Y and Tb to Lu contents of the Kronotsky peridotites are several times higher than those of the Mt. Soldatskaya peridotites. i.e., in regard to Y and the HREE, the Kronotsky peridotites are transitional between patterns of

supra-subduction zone ophiolites and mid oceanic ridge mantle residues. The distribution of stable elements Y and HREE may hint at the history of the rocks before this metasomatism.

The gabbro-pegmatites, forming dikes in peridotites, show broad chemical variations due to changing proportions of mafic and felsic minerals: 5.3–9.0% MgO, 2.15–4.29% Na₂O, 14.0–23.0% Al₂O₃, and 7.5–14.0% CaO (Table 3). The REE patterns of the pyroxenites and gabbro-pegmatites are similar to peridotitic ones, but REE totals in the former are slightly higher. This indicates that these rocks, occurring among these peridotites, crystallized from melts similar to primary ones, derived from peridotite melting. The gabbro-pegmatites have positive Eu-anomalies indicating plagioclase predominance; the pyroxenite shows negative Eu-anomaly. (Fig. 5c). The gabbroic rocks, very coarse crystalline gabbros and gabbro-dolerites, differ distinctly from those of the Olenegorsk Pluton in terms of magnesium, sodium, potassium, and titanium contents (4.5–5.0% MgO, 3.25–4.2% Na₂O, 0.66–1.22% K₂O, 0.51–0.79% TiO₂) (Table 3). These differences are due partly to secondary alteration since the REE patterns of the gabbro-diabase are similar to those of the gabbros crystallized from depleted oceanic tholeiites. However, the REE pattern of the very coarse crystalline gabbros with higher potassium contents rises gradually from HREE to LREE, probably indicating derivation from enriched melts (Fig. 5c). Basalts from the serpentinite mélange of the Kronotsky Peninsula are chemically similar to N-MORB derivatives (see Fig. 10) (Skolotnev *et al.* 2003; Saveliev 2004). Dolerites (blocks from the serpentinite melange) have similar chemistry as the basalts. However, they are more depleted than the basalts and have particularly lower Al, high field strength elements (HFSE) like Nb, Ta, Hf and Ti, whereas the LILE, Th and Ba are increased relatively to Nb and Ta (Table 3) (Fig. 10b).

MINERAL CHEMISTRY

OPHIOLITES OF THE SOUTHERN KAMCHATSKY MYS PENINSULA

Mt. Soldatskaya Massif. Mineral composition of the ultramafic rocks remains the same through out the sequence, in the peridotites and serpentinites alike. The clinopyroxene (Fs₃₋₄) has 0.6–1.16% Cr₂O₃, 1.44–2.54% Al₂O₃, and 0.01–0.02% Na₂O; the orthopyroxene (Fs₈₋₉) has 0.5–0.73% Cr₂O₃, 1.37–1.99% Al₂O₃, and 0–0.01% Na₂O; the olivine has Fo_{90,9-91,7}; and the spinel has Cr# = 47–70, Mg# = 53–60, and 0.01–0.02% TiO₂. The mineral composition signatures, according to Hebert *et al.* (1989), indicate that these peridotites are of restite origin. The two-pyroxene thermometry yielded crystallization temperature of 920°C. Both the high values of Cr# (Cr# = Cr/Cr+Al) of spinel and the Al₂O₃ content of orthopyroxenes enable a comparison with the subduction margin field (Kay & Senechal 1976; Bloomer & Hawkins 1983; Bonatti & Michael 1989) (Fig. 11).

Olenegorsk Pluton. Clinopyroxene in diallage gabbros is characterized by Fs₉₋₁₂, Wo₄₄₋₄₆ and En₄₂₋₄₆, with oxides ranging as follows: 0.46–0.78% TiO₂, 2.57–2.96% Al₂O₃, 0.07–0.17% Cr₂O₃, and 0.31–0.41% Na₂O. Orthopyroxenes have Fs₂₇₋₃₀, Wo_{2.8-3.6}, En₆₅₋₆₉, with oxides varying as follows: 0.38–0.74% TiO₂, 1.46–1.59% Al₂O₃, 0.04–0.05% Cr₂O₃. Plagioclase is labradorite (An₅₅₋₆₂). Clinopyroxene compositions on the TiO₂ vs. FeO/MgO diagram (Zlobin & Zakariadze 1985) plot in the field of clinopyroxenes from gabbroic rocks formed in mid-ocean ridges (Fig. 7b). The rare grains of spinel have Cr# = 57, Mg# = 31, and 1.40% TiO₂. At the contact with serpentinite, the rock-forming minerals in the gabbros change in composition. The clinopyroxene becomes higher in Cr (0.30% Cr₂O₃) and Mg (Fs₁₀₋₁₆), but lower in Ti (0.54% TiO₂) and Al (2.57% Al₂O₃); the plagioclase becomes more calcic (An_{77.5}).

The clinopyroxene from the schlieren composed of olivine gabbro-norite has higher Cr (0.55–0.58% Cr₂O₃) and Mg (17–18% MgO) and lower calcium (17–18% CaO) and titanium (0.52–0.59 TiO₂) contents than clinopyroxene outside the schlieren (0.06–0.12% Cr₂O₃, 14–16% MgO, 21–22% CaO, 0.70% TiO₂). Similar features are typical of the

orthopyroxene: Cr₂O₃ (0.21%) MgO (29%) in orthopyroxene from the schlieren and Cr₂O₃ (0.02–0.05%), MgO (24%) in orthopyroxene outside the schlieren. The plagioclase from the schlieren segregations is more calcic An_{78–82} than plagioclase outside the schlieren An_{55–64}. The olivine has Fo₈₀, and the composition of spinel is characterized by Cr# = 47, Mg# = 36, and 0.56% TiO₂.

Compared to the spinels from Mt. Soldatskaya peridotites, the spinels in the serpentinite enclaves from the gabbros are substantially more ferroan (Mg# = 20–48) and more chromian (Cr# = 43–64). They show extremely strong and non-systematic titanium enrichment (0.23–7.99% TiO₂). Pyroxene compositions in serpentinite enclaves are similar to those in the harzburgites and serpentinites of the Mt. Soldatskaya Massif, showing clinopyroxene of Fs_{2.9–4.2}, Wo_{45–47}, En_{48–51}, 0–0.04% TiO₂, 2.42–2.68% Al₂O₃, and 1.04–1.19% Cr₂O₃, and orthopyroxene of Fs_{8.5–9}, Wo_{1.99–2.12}, En_{84–89}, 0–0.03% TiO₂, 1.81–1.90% Al₂O₃, and 0.57–0.75% Cr₂O₃. Olivine composition in the serpentinite enclaves is characterized by lower Fo (Fo₈₈) but close to that of the Mt. Soldatskaya harzburgites.

The above features of the Cr-spinels and serpentinite textures in the ophiolite associations and oceanic peridotites were repeatedly described in literature and interpreted to result from impregnation of peridotites by mafic melts (Seyler & Bonatti 1997; Bonatti *et al.* 1992; Tartarotti & Vaggelli 1995). If this is the case, then the Mt. Soldatskaya peridotites and serpentinite enclaves in the gabbroic rocks have common nature, yet the latter suffered chemical and structural transformation under the influence of mafic melt.

In all rock types, the layered series of the Olenegorsk Pluton olivine (Fo_{84–86}) is mostly replaced by serpentine, whereas the plagioclase (An_{80–82}) is partly or completely replaced by chlorite, hydrogrossular and prehnite. Spinel compositions (Cr# = 49–65, Mg# = 34–45) from the rocks of the layered series are similar to that from the serpentinite enclaves, which are widespread among the gabbroic rocks of this pluton. Spinel compositions show strong and extremely irregular titanium enrichment (0.96–5.02% TiO₂). The clinopyroxene

(Fs₆₋₈) shows non-systematic TiO₂ enrichment (0.34–1.72%); coincidentally, the Cr₂O₃ contents (0.31–1.30%) are equal to those in Mt. Soldatskaya peridotites. The TiO₂ contents (0.30–0.35%) in the orthopyroxene (Fs₈₋₉) are the same as in the orthopyroxene from the gabbro; and the Cr₂O₃ contents (0.40–0.45%) are the same as in the peridotites.

The structural features of the studied fragments of the layered series, compositional signatures of the spinels and clinopyroxenes (enriched in basaltic melt components), the rock textures with xenomorphic plagioclase and clinopyroxene segregations among olivines, possibly indicate that the rocks of the layered series are produced by interaction between mafic melts and peridotites similar to Mt. Soldatskaya harzburgites. This assumption is supported by the similarity of spinel and clinopyroxene compositions and of rock Cr# of layered series and ultramafic rocks of the Mt. Soldatskaya Massif.

Olkhovaya Gabbro Block. Pyroxenes from the gabbro differ from those of the Olenegorsk Pluton, which are similar to derivatives of oceanic tholeiites in terms of bulk rock chemistry and trace element contents. The former are lower in titanium (0.19–0.24% TiO₂ in Cpx and 0.16% TiO₂ in Opx), chromium (0.02–0.09% Cr₂O₃ in Cpx and 0.02% in Opx), and aluminum (1.22–1.39% Al₂O₃ in Cpx and 1.25% in Opx). The plagioclase is more calcic: An₇₇₋₈₂. Clinopyroxene compositions on the TiO₂ vs FeO/MgO diagram (Zlobin & Zakariadze 1985) plot in the field of clinopyroxenes from gabbroic rocks formed in supra-subduction zone setting (Fig. 7b).

OPHIOLITES OF THE EASTERN KRONOTSKY PENINSULA

Mineral compositions that we have studied from the harzburgites show only slight variations. Clinopyroxene (Fs₄₋₅) has 0.03–0.07% TiO₂, 3.39–4.60% Al₂O₃, and 1.02–1.34% Cr₂O₃; orthopyroxene (Fs₁₀₋₁₁) has 0.03–0.07% TiO₂, 3.33–3.70% Al₂O₃, and 0.63–0.81% Cr₂O₃; olivine has Fo₉₀; and spinel has Mg# = 67–70 and Cr# = 23–32. These features show that these peridotites are similar to the moderately depleted restites widespread in mid-ocean ridges. In this sense, the most convincing evidence is provided

by the spinel Cr# and the orthopyroxene Al_2O_3 contents. Two-pyroxene thermometry shows equilibration temperatures of about 945°C.

The clinopyroxenes from the gabbro-diabase (Fs_{12-20}) have 0.11–0.26% TiO_2 , 0.87–2.09% Al_2O_3 , and 0.06–0.24% Cr_2O_3 ; the plagioclase has An_{60-80} . Clinopyroxene porphyroclasts in the augen-gabbro are more magnesian and calcic than those in the gabbro-dolerites; the plagioclase is more calcic (An_{90}). The neoblast and porphyroclast compositions of the clinopyroxene and plagioclase are similar. The olivine neoblast composition is Fo_{78} . On the TiO_2 vs FeO/MgO diagram after (Zlobin and Zakariadze 1993), these clinopyroxene compositions plot in the field of clinopyroxenes formed in supra-subduction zone setting (Fig. 7b).

The preserved relicts of minerals from the gabbro-pegmatites (gabbro-norites) have the following compositions: plagioclase has An_{90} ; clinopyroxene has Fs_{25-30} , 0.04% TiO_2 , 1.39% Al_2O_3 , and 0–0.01% Cr_2O_3 , and orthopyroxene has Fs_{40-45} , 0.05–0.08% TiO_2 , 0.99–2.11% Al_2O_3 , and 0–0.11% Cr_2O_3 . This compositional feature, very calcic plagioclase coexisting with highly ferroan pyroxenes, may suggest that primary melts for the gabbro-pegmatites were high-Al basalts, which also have high Fe contents (Khubunaya 1987).

GEODYNAMIC SETTING AND CONCLUSIONS

Our study shows that the rocks attributed to the ophiolite assemblage based on geological, geochemical, and mineralogical evidence constitute several ophiolitic complexes of different origins.

(1) Aptian–Cenomanian complex: a fragment of ancient oceanic crust, composed of tholeiite basalts, pelagic sediments, and gabbroic rocks, presently occurring in distinct tectonic slices (Afrika Complex) and in olistolithes in Pikezh complex of the Kamchatsky Mys Peninsula and probably in mélangé of the Kronotsky Peninsula.

(2) Upper Cretaceous complex, composed of highly depleted peridotite, gabbro, and plagiogranite, associated with island arc tholeiite, boninite, and high-alumina tholeiitic basalt of supra-subduction origin;

(3) Paleocene–Early Eocene complex of intra–island arc or backarc origin, composed of gabbros, dolerites (sheeted dikes) and basalts produced from oceanic tholeiite melts, and BAB-like dolerites.

Formation of distinct ophiolite complexes is related to the Kronotskaya intraoceanic volcanic arc evolution. According to paleomagnetic data on the Upper Cretaceous and Paleocene formations, which outcrop on the Kronotsky and Kamchatsky Mys Peninsulas, the Kronotsky arc was formed at 20° N and had W-E extension (Bazhenov *et al.* 1992; Pechersky *et al.* 1997; Levashova 2000). Subduction zone was located to the south from the arc and initiated since Late Cretaceous time (Alekseev *et al.* 2006).

The first ophiolite complex is a fragment of ancient oceanic crust on which the Kronotskaya arc originated. At the Kamchatsky Mys Peninsula, it is represented by jaspers and limestones of Aptian–Cenomanian age that interbedded with the N-MORB-like tholeiitic basalts (the Afrika Complex). These basalts were formed in mid-ocean ridge setting and most likely are fragments of the Kula or Pacific oceanic plates. At the Kronotsky Peninsula basalts from serpentinite mélangé are chemically similar to N-MORBs. Their age is unknown. Based on the geochemistry, these basalts are comparable with N-MORBs of the Aptian-Cenomanian Afrika complex. Island arc volcanism within the Kronotskaya arc was initiated since Koniacian–Campanian age until Middle Eocene. During that time, the subduction of Kula or Pacific plate beneath the arc took place. This plate moved northward until Middle Eocene (Engelbreton *et al.* 1987). The formation of the second and third ophiolite complexes are correlated with the Kronotskaya arc evolution (Fig 12).

The peridotites of the second ophiolite complex, on the basis of their mineral composition and chemistry, are restites after partial melting of depleted mantle. The

peridotite spinels from the Mt. Soldatskaya Massif (Kamchatsky Mys Peninsula) are highly chromian, plotting outside the field of oceanic peridotites and they fall in the field of subduction margins that include the Mariana Trench peridotites (Bloomer & Hawkins 1983) in the spinel $100 \text{ Cr}/(\text{Cr}+\text{Al})$ vs Al_2O_3 diagram after Bonatti and Michael (1989). The REE patterns of the peridotites of the Kamchatsky Mys ophiolite association show good conformity with those of the Troodos ophiolite, which was generated above a subduction zone (Kay & Senechal 1976; Bloomer & Hawkins 1983; Bazylev *et al.* 1993; Sobolev *et al.* 1993; Bloomer *et al.* 1995).

The fine-grained gabbro with plagiogranite from the source region of the Pervaya Olkhovaya River may be attributed to the same supra-subduction ophiolite complex. Plagiogranite occurring in fine veins and dike-like bodies in the gabbroic rocks shows that they formed at the late stage of gabbro emplacement. The presence of angular gabbroic xenoliths in plagiogranite confirms that the plagiogranites crystallized later than the Olkhovaya gabbro (Fig. 3). The above trace element data for the plagiogranites (negative Ta, Nb anomalies; Rb vs. Y+Nb interrelation) and the low TiO_2 , Zr, and Y contents of the gabbroic rocks along with their mineral compositions lead to the conclusion that these rocks were formed in supra-subduction zone (SSZ) setting. However some of the REE patterns in the gabbroic rocks and some plagiogranites are similar to those of oceanic tholeiites. From the chemical and mineralogical data, it appears most likely that the gabbroic rocks and plagiogranites are derivatives of island arc tholeiitic melts. The plagiogranite melt was residual in the process of parental tholeiitic magma fractionation, and at later stages it was squeezed out of the magma chamber. Geochemical modeling shows that LREE depleted plagiogranites may result from 70–80% fractional crystallization of gabbroic liquid (Fig. 6b). The average U-Pb SHRIMP zircon dating of plagiogranite according to 7 points is 74.7 ± 1.8 M.a. (Luchitskaya *et al.*, 2006). Cathodoluminescence spectra of zircons show oscillatory zoning and the absence of xenogenic cores, which

indicate magmatic origin of zircons. Thus the intrusion and crystallization of plagiogranites occurred in Campanian time.

At the Kamchatka Mys Peninsula, we put together in one complex the peridotites of Mt. Soldatskaya, abbroic rocks and plagiogranites of Pervaya Olkhovaya River based on their SSZ geochemistry and mineralogy. We propose that Campanian age of plagiogranites allow us to refer the formation of supra-subduction ophiolite complex to Upper Cretaceous time. In this case we suggest that in the Kamchatsky Mys Peninsula, only Upper Cretaceous boninites (Fedorchuk 1992) and island arc tholeiites in the lower part of the Tarkhovskaya Formation (within the Stolbovskoy block) may be cogenetic with the supra-subduction zone peridotites.

The mineral chemistry data suggest similarity of the Kronotsky Peninsula peridotites to moderately depleted restites widespread in mid-ocean ridges (Bonatti and Michael 1989). Most meaningful in this respect are the high Al contents of the spinels and orthopyroxenes (Fig. 11). However HREE contents in peridotites are distinctly lower than those in mid-oceanic ridge mantle residues (MOMR). Moreover, the LREE patterns of the peridotites and of their cogenetic pyroxenite and gabbro-pegmatite dikes point to a cryptic metasomatic imprint above the subducting plate. Therefore, these peridotites may have formed as oceanic rift residues and suffered depletion and slab-induced metasomatic imprint after transport in a subduction zone position (Kramer *et al.* 2001). Skolotnev *et al.* (2003) supposed an origin of these peridotites directly within the SSZ area, assuming that widespread at Kronotsky Peninsula plagioclase-bearing tholeiites of Coniacian-Campanian-Maastrichtian Kamenistskaya Formation are cogenetic to these peridotites. According to (Khubunaya 1987) plagioclase-bearing tholeiites were formed from high-Al tholeiite melts at the initial stages of intraoceanic arc evolution. The gabbroic rocks and amphibolites from blocks in serpentinite mélangé with low-TiO₂, low-Al₂O₃ clinopyroxenes might be fragments of the same complex. The age of the SSZ Kronotsky ophiolite complex may be construed as pre-Eocene because serpentinite fragments occur in the

conglomerates of the Kronotskaya (Middle Eocene) Group. If our suggestion that Kamenistskaya Formation basalts and peridotites are cogenetic is true, then the age of this ophiolite complex is Coniacian-Maastrichtian.

According to our data ophiolites of SSZ nature related to the Kronotskaya paleoarc at the Kamchatsky Mys and Kronotsky Peninsulas were formed approximately simultaneously in Upper Cretaceous time and are the fragments of a single ophiolite complex. This ophiolite complex was formed as a result of repeated partial melting of a peridotites in the mantle wedge with production of tholeiite basalts and boninites in the Kamchatsky Mys segment and plagioclase-bearing tholeiites in the Kronotsky segment (fig 12) (Kramer et al 2001).

Further evolution of Kronotskaya volcanic arc resulted in extension within the arc and formation of the third ophiolite complex with intra-arc and MORB geochemical characteristics. The beginning of extension was probably initiated by the Kula-Pacific spreading ridge subduction. The Olenegorsk Pluton gabbro and dike complex were formed in Paleocene-Eocene and along with the eruption of the Kamensk complex basalts and accumulation of pelagic and hemi-pelagic deposits took place (Skolotnev *et al.* 2001).

The gabbroic rocks of the Olenegorsk Pluton contain ultramafic xenoliths, which are significantly higher in all REE, Ti, Zr, and lower in Mg than Mt. Soldatskaya pluton spinel peridotites. However some spinel and clinopyroxene compositions are similar to those of peridotites of Mt. Soldatskaya pluton. Numerous examples of mafic magma influence on ultrabasic composition are described for ophiolite complexes and oceanic lithosphere (Tartarotti & Vaggelli. 1995, Tartarotti *et al.* 2002, in particular). During interaction between mafic magma and ultrabasic rocks the spinel and clinopyroxene composition changes in the same manner as in the case of ultramafic xenoliths of the Olenegorsk Pluton. Therefore, the gabbroic rocks of the Olenegorsk Pluton could not have formed earlier than the peridotites of Mt. Soldatskaya pluton, i.e., earlier than Late Cretaceous.

Geologic data indicate that formation of Olenegorsk Pluton gabbro and dolerites occurred after formation of Upper Cretaceous complexes of island arc nature (gabbro contains xenoliths of peridotites which have suprasubduction nature). Paleocene-Early Eocene brown mudstones and siltstones of Kamensk complex contain lense-like interlayers of breccias and microbreccias with clasts of gabbro, diabase and basalts, rare jaspers and limestones (Fedorchuk, 1992). Taking into account that gabbro and dolerites of Olenegorsk Pluton as well as basalts of the Kamensk Complex represent the product of tholeiites melts of N-MORB type, we combine gabbros and dolerites of the Olenegorsk Pluton and the Kamensk basalts in a single ophiolite assemblage. Basalts of the Kamensk complex and associated Paleocene-Early Eocene sedimentary formations represent upper members of this ophiolite assemblage. Thus we suppose that this complex has Paleocene-Early Eocene age. Based on their geochemical signatures, it might have formed either in mid-ocean ridge or in back-arc setting. However, because the gabbro contains peridotite xenoliths similar to those from Mt. Soldatskaya Pluton, formed in supra-subduction zone setting, it is obvious that the pre-Middle Eocene ophiolite complex originated near or inside a volcanic arc (Skolotnev *et al.* 2001). The existence of a “dike complex” in the Olenegorsk Pluton indicates that it formed in an extensional setting, with the direction of dike extension being roughly parallel to the axis of the spreading center (Tsukanov *et al.* 2004). At the Kronotsky Peninsula, dolerites are observed as blocks in serpentized mélangé where some dolerites exhibit characteristics similar to BABBs (fig. 10b). This fact indicates that an intra-arc spreading center may have existed in this region. One can suppose that a similar spreading center existed within the Kamchatsky Mys segment of the Kronotskaya arc in Paleocene-Early Eocene time. The Kronotsky Peninsula basalt and dolerite ages demand further investigations. The geodynamic setting of Paleocene-Middle Eocene time may be compared with the modern Mariana island arc in the Philippine sea (Hawkins *et al.* 1990; Fedorchuk 1992; Ishiwatari *et al.* 2003). Reorganization of oceanic plates and change in the direction of the Kula and Pacific

movement during the Middle Eocene resulted in cessation of active subduction beneath the Kronotskaya arc (Engebretson *et al.* 1987; Kononov 1989). During this time a new subduction zone of northwestern polarity beneath Kamchatka margin, where the Vetlovsky marginal basin crust subducted, was initiated (Fig. 12b) (Alekseev *et al.* 2006). This was followed by Middle Eocene volcanism within the Kronotskaya arc, probably, related to the residual magmatic chamber in the arc basement. OIB and MORB magmatism occurred related to the spreading zone within the intra arc setting similar to what is recognized elsewhere (Shervias 2000) (fig. 12b).

The beginning of Kronotskaya arc collision with Kamchatka margin is dated Late Eocene, which correlates well with the deformation episode in structure of Kronotsky terrane, related to shortening subperpendicular to the arc extension. This tectonic episode is correlated with the blocking of the subduction zone beneath the Kronotskaya arc as a result of spreading ridge merging (Alekseev *et al.* 2006). Formation of Kronotsky terrane modern structure occurred in Oligocene – Early Miocene, and at the Kamchatsky Mys Peninsula it continues at the present time (Gaedicke *et al.* 2001; Freitag *et al.* 2003).

Acknowledgments

We express our gratitude to Dr. A.V. Fedorchuk and Dr. D.P. Saveliev for fruitful discussion and Dr. I.R. Kravchenko-Berezhnoy for his help in translating this paper. Prof. J. Erzinger and coworkers in the geochemical laboratory of the Geoforschungszentrum Potsdam and Prof. D.Z. Zhuravlev (Institute of Mineralogy and Geochemistry of Trace Elements, Moscow) are thanked for trace- and major-element analysis. We also express our gratitude to the reviewers whose remarks led to the improvement of this manuscript. This work was supported by the Russian Foundation for Basic Research (project nos. 01-05-64469, 02-05-64060, 04-05-65132, 05-05-64158) by the German Ministry for Science and Research (BEO-Grant 03F16GUS).

References

- ALEXEIEV D.V., TSUKANOV N.V., LEWERENZ S., FREITAG R., GAEDICKE C. & HOLL H.G. 1999. Middle Eocene collision of the Kronotskiy terrane with Kamchatka: new evidence from provenance analysis of the Upper Eocene to Middle Miocene Tyushevka sandstones. *AGU Fall Meeting EOS Transactions*, F953-F954.
- ALEXEIEV D.V., GAEDICKE C., TSUKANOV N.V. & FREITAG R. 2006. Collision of the Kronotskiy arc at the NE Eurasia margin and structural evolution of the Kamchatka-Aleutian junction. *International Journal. Earth Sciences*, **vol 95**, 6, 977-994.
- BAZYLEV B.A., MAGAKYAN R., SILANT'EV S.A., IGNATENKO K.I., ROMASHOVA T.V. & KSENOFONTOS K. 1993. Petrology of ultrabasic rocks of Mamoniaya complex, southwestern Cyprus. *Petrology* **1**, 348-378.
- BAZHENOV M.L., BURTMAN V.S., KREZHOVSKIKH O.A. & SHAPIRO M.N. 1992. Paleomagnetism of Paleogene rocks of the Central-East Kamchatka and Komandorsky Islands: tectonic implications. *Tectonophysics* **201**, 157-173.
- BENIYAMOVSKY V.N., FREGATOVA N.A., SPIRINA L.V., *et al.* 1992. Zonation of the planctonic and benthonic foraminiferas in the Paleogene of the Eastern Kamchatka. *News USSR Academy of Science, Geological. Series. 1*, 100–113. (in Russian).
- BLOOMER S.H. & HAWKINS J.W. 1983. Gabbroic and ultramafic rocks from Mariana trench: an island arc ophiolite. In Hayers D.E. (ed.) *The Tectonic and Geologic Evolution of Southeast Asia Seas and Islands*. (Pt 2). *Geophysical Monograph*, **vol 27**, pp. 294-317. AGU, Washington, D.C.
- BLOOMER S.H., TAYLOR B., MACLEOD C. J. *et al.* 1995. Early arc volcanism and the ophiolite problem: a perspective from drilling in the Western Pacific. In Taylor B. & Natland, J. (eds.) *Active Margins and Marginal Basins of the Western Pacific*. *Geophysical Monograph*, **88**, pp. 1-30. American Geophysical Union, Washington, DC.
- BONATTI E. & MICHAEL P. J. 1989. Mantle peridotites from continental rifts to oceanic basins to subduction zones. *Earth and Planetary Science Letters* **91**, 297-311.
- BONATTI E., PEYVE A., KEPEZHINSKAS P. *et al.* 1992. Upper mantle heterogeneity below the Mid-Atlantic Ridge, 0°–15° N. *Journal of Geophysical Research* **97**, **B4**, 4461-4476.
- BOYARINOVA M.E., VESHNYAKOV N.A., KORKIN A.G. & SAVELIEV D.P. 2000. State geological map of Russian Federation, scale 1:200000. Series Eastern Kamchatka. Papers O-58-XXVI, XXXI, XXXII (second edition). Explanatory report. Saint-Petersburg.
- BOYARINOVA M.E., VESHNYAKOV N.A., KORKIN A.G., SAVELIEV D.P. & LITVINOV A.F. 2001. State geological map of Russian Federation, scale 1:200000. Series Eastern

- Kamchatka. Papers N-57-XII, N-58-VII, N-57-XVIII (second edition). Explanatory report. Saint-Petersburg.
- ENGBRETSON D.C., COX A. & GORDON R.G. 1987. Relative motions between oceanic and continental plates in the Pacific Basin. *Geological Society of America. Special Paper* **206**, 59 p.
- EVENSEN N.M., HAMILTON P.J. & O' NIONS R.K. 1978. Rare earth abundances in chondritic meteorites. *Geochimica et Cosmochimica Acta* **42**, 1199-1212.
- FEDORCHUK A.V. 1989. Ophiolites of the Kamchatsky Mys peninsula (Eastern Kamchatka). *Ofioliti* **14**, 1/2, 3-12.
- FEDORCHUK A. V. 1992. Oceanic and back-arc basin remnants within accretionary complexes: Geological and Geochemical evidences from the eastern Kamchatka. *Ofioliti* **17**, 219–242.
- FREITAG R., GAEDICKE C., BARANOV B., & TSUKANOV N. 2001. Collisional processes at the junction of the Aleutian-Kamchatka arcs: New evidence from fission track analysis and field observation. *Terra Nova* **13**, 433-442.
- GAEDICKE C., BARANOV B.V., SELIVERSTOV N.I., ALEXEIEV D.V., TSUKANOV, N.V. & FREITAG R. 2000. Structure of an active arc-continent collision area: the Aleutian - Kamchatka junction. *Tectonophysics* **325**, 63 – 85
- GEIST E.L., VALLIER T.L., SCHOLL D.W. 1994. Origin transport and emplacement of an exotic island-arc terrane exposed in eastern Kamchatka, Russia. *Geological. Society. of America. Bulletin.* **106** (9), 1182-1194.
- HAWKINS J.W., LONSDALE P.F., MACDOUGAL J.D. & VOLPE A.M. 1990. Petrology of the axial ridge of the Mariana Trough backarc spreading center. *Earth and Planetary Science Letteres* **100**, 226-250.
- HEBERT R., SERRI G. & HEKINIAN R. 1989. Mineral chemistry of ultramafic tectonites and ultramafic to gabbroic cumulates from the major oceanic basins and Northern Apennine ophiolites (Italy) – A comparison. *Chemical Geology* **77**, 183-207.
- HOFMANN A.W. 1988. Chemical differentiation of the Earth: the relationship between mantle. Continental crust and oceanic crust. *Earth and Planetary Science Letters* **90**, 243-262.
- ISHIWATARI A. , SOKOLOV S.D. & VYSOTSKY S.V. 2003. Petrological diversity and origin of ophiolites in Japan and Far East Russia with emphasis on depleted harzburgite. In Dilek Y. and Robinson P.T. (eds.) *Ophiolites in Earth's history. Geological Society London. Special Publication* **218**, 597-617.
- KAY R. W. & SENECHAL R. G. 1976. The rare earth geochemistry of the Troodos ophiolite complex. *Journal of Geophysical Research* **81**, 5 964-970.

- KONONOV M.V. 1989. Plate tectonics of the Northwest Pacific. Moscow, Nauka Publishers. 168 p. (in Russian).
- KHOTIN M.Yu. 1976. Effusive-tuff-siliceous formation of the Kamchatka Cape. Moscow, Nauka Publishers. 196 p. (in Russian).
- KHUBUNAYA S.A., 1987. High alumina plagioclase-tholeiitic formation of island arcs, 168 p. Moscow, Nauka Publishers (in Russian).
- KONSTANTINOVSKAIA E.A. 2001. Arc – continent collision and subduction reversal in the Cenozoic evolution of the North-West Pacific: An example from the Kamchatka (NE Russia). *Tectonophysics. Active Subduction and collision in South-East Asia (SEASIA)*. Spec. Is. **333**, 1/2, 75-94
- KRAMER W., SKOLOTNEV S.G., TSUKANOV N.V. *et al.* 2001. Geochemistry, mineralogy and geological framework of basic-ultrabasic complexes on the Kamchatka Cape Peninsula. In Karpov G.A., Kozlov A.P., Osipenko A.B. and Sidorov E.G. (eds.) *Petrology and Metallogeny of the Kamchatka mafic-ultramafic complexes*, pp. 170-191, Scientific World, Moscow. (in Russian).
- LEVASHOVA N.M., SHAPIRO M.N., BEN'YAMOVSKII V.N. & BAZHENOV M.L. 2000. Paleomagnetism and geochronology of the Late Cretaceous - Paleogene island arc complex of the Kronotsky peninsula, Kamchatka, Russia: kinematic implications. *Tectonics* **19**, 5, 834-851.
- LUCHITSKAYA M.V., TSUKANOV N.V., SKOLOTNEV S. G. 2006. New SHRIMP U–Pb zircon data from plagiogranites of Kamchatsky Mys ophiolite assemblage (Eastern Kamchatka). *Transactions Russian Academy of Science, Earth Science Section* **408**, 4, 869-875.
- MARKOVSKY B.A. & ROTMAN V.K. 1981. Geology and Petrology of the ultramafic volcanism, 245 p. Nedra, Leningrad. (in Russian).
- NOKLEBERG W.J., PARFENOV L.M., MONGER J.W. , *et al.* 1994. Circum-North Pacific tectono-stratigraphic terrane map. U.S. Department of the Interior. U.S. Geological Survey. *Open file report* , v. **94**.
- OSIPENKO A.B. & ANOSOV G.I. 2002. Ultramafic rocks of the Rakovaya Bay (Eastern Kamchatka); composition and geodynamic tips. *Geology and Geophysics* **43**, 858-872. (in Russian).
- PARFENOV L.M., NATAPOV L.M., SOKOLOV S.D. & TSUKANOV N.V. 1993. Terrane analysis and accretionary in North-East Asia. *The Island Arc* **2**, p. 35-54.
- PECHERSKY D.M., LEVASHOVA N.M., SHAPIRO M.N., BAZHENOV M.L. & SHARAPOVA Z.V. 1997. Paleomagnetism of Paleogene volcanic series of the Kamchatsky Mys peninsula, Eastern Kamchatka: the motion of an active island arc. *Tectonophysics* **273**, 219-237.

- PEARCE J.A., HARRIS N.B.W. & TINDLE A.G. 1984. Trace element discrimination diagrams for the tectonic interpretation of granitic rocks. *Journal of Petrology* **25**, 956-983.
- PEYVE A.A. 1987. Hyperbasites of the Kamchatka Cape Peninsula (Eastern Kamchatka). *Pacific Geology* **2**, 41-46. (in Russian).
- RAMPONE E., HOFMANN A. W., PICCARDO G. B., VANNUCCI R., BOTTAZZI P. & OTTOLINI L. 1996. Trace element and isotope geochemistry of depleted peridotites from an N-MORB type ophiolite (Internal Liguride, N. Italy). *Contribution of Mineralogy and Petrology* **123**, 61-76.
- RAZNITSYN YU.N., KHUBUNAYA S.A. & TSUKANOV N.V. 1985. Tectonics of the eastern part of the Kronotsky peninsula, and formational types of basalts (Kamchatka). *Geotectonics* **1**, 88-101. (in Russian).
- ROLLINSON H.R. 1994. Using geochemical data: evaluation, presentation, interpretation. Essex: London Group UK Ltd. 352 p.
- SAUNDERS A.D. & TARNEY J. 1984. Geochemical characteristics of basaltic volcanism within back-arc basins. In Kokelaar B.P. and Howells M.F. (eds.) *Marginal basin geology*, pp. 59-76, Special Publication **16**, Geological Society, London.
- SAVELIEV D.P. 2004. Within-plate volcanics in the Cretaceous oceanic complexes of Eastern Kamchatka. *PhD Thesis*, 23 p. (in Russian).
- SEYLER M. & BONATTI E. 1997. Regional-scale melt-rock interaction in lherzolitic mantle in the Romanche Fracture zone Atlantic Ocean. *Earth and Planetary Science Letters* **146**, 273-287.
- SHAPIRO M.N., ERMAKOV V.A., SHANTSER A.E., SHUL'DINER V.I., KHANCHUK A.I. & VYSOTSKIY S.V. 1987. Tectonic evolution of Kamchatka. 248 p. Moscow, Nauka Publishers (in Russian).
- SHCHERBININA E.A. 1997. Nannoplankton from the Paleogene rocks in the eastern Kamchatka region. *Stratigraphy and Geological Correlation* **5**, 2, 60-70.
- SHERVAIS J.W. 2001. Birth, death, and resurrection: The life cycle of suprasubduction zone ophiolites. *Geochemistry, Geophysics, Geosystems* **2**, 2000GC000080.
- SKOLOTNEV S.G., KRAMER W., TSUKANOV N.V. *et al.* 2001. New data on the origin of the ophiolites in the Kamchatskii Mys Peninsula (NE Kamchatka). *Transactions Russian Academy of Science, Earth Science Section* **381**, 8, 881-883.
- SKOLOTNEV S.G., KRAMER W., TSUKANOV N.V., SEIFERT W., FREITAG R. & SAVELIEV D. 2003. The heterogeneity of ophiolite association in the Kronotsky paleoarc basement (Eastern Kamchatka). *InterRidge News* **12**, 1 30-34.
- SOBOLEV A.V., PORTNAYAGIN M.V., DMITRIEV L.V. *et al.* 1993. Petrology of ultramaphic lavas and association rocks of Troodos massif, island Cyprus. *Petrology* **1**, 379-412.

- SOKOLOV S.D., BYALOBZHEBSKII S.G., 1996. Terranes of the Koryak highlands, Northeastern Russia. *Geotectonics* **6**, 68 – 80. (in Russian).
- SUN S.S. & McDONOUGH W.F. 1989. Chemical and isotopic systematics of oceanic basalts: implications for mantle composition and processes. In Saunders A.D. and Norry M.J. (eds.) *Magmatism in the ocean basins*, pp. 313-345, Special Publication **42**, Geological Society, London.
- TARTAROTTI P., SUSINI S., NIMIS P., OTTOLINI L. 2002. Melt migration in the upper mantle along the Romanche Fracture Zone (Equatorial Atlantic). *Lithos* **63**, 125-149.
- TARTAROTTI P. & VAGGELLI G. 1995. Melt impregnation in mantle peridotites and cumulates from the Elba island ophiolites, Italy. *Memorie di Scienze Geologiche* **47**, 201-215.
- TSUKANOV N.V., FEDORCHUK A.V. & LITVINOV A.F. 1991. Oceanic complexes in the structure of Shipunsky Peninsula, Eastern Kamchatka. *Transactions Russian Academy of Science, Earth Science Section* **318**, 4, 958-962.
- TSUKANOV N.V. & FEDORCHUK A.V. 2001. Ophiolite complexes in accretionary structure of the Eastern Kamchatka. In Karpov G.A., Kozlov A.P., Osipenko A.B. and Sidorov E.G. (eds.) *Petrology and Metallogeny of the Kamchatka mafic-ultramafic complexes*, pp. 159-169, Scientific World, Moscow. (in Russian).
- TSUKANOV N.V., LUCHITSKAYA M.V., SKOLOTNEV S.G., KRAMER W. & SEIFERT W. 2004. New data on the structure and composition of the gabbroides and plagiogranites from the Late Cretaceous ophiolite complex, Kamchatsky Mys Peninsula, Eastern Kamchatka. *Transactions Russian Academy of Science, Earth Science Section*. **397**, 2, 243-246. (in Russian).
- VYSOTSKIY S.V. 1989. Ophiolite associations of the island arc systems of the Pacific Ocean. 195 p. Far Eastern Department of USSR Academy of Science, Vladivostok. (in Russian).
- WATSON B.F. and FUJITA K. 1985. Tectonic evolution of Kamchatka and sea of Okhotsk and implication of the Pacific Basin. In: Howell D.G. (ed.). *Tectonostratigraphic terranes of the Circum - Pacific Region. 1. Circum – Pacific Council for Energy and Mineral Resources*. Houston, pp. 333-348
- ZINKEVICH V.P., KAZIMIROV A.D., PEYVE A.A. & CHURAKOV G.M. 1985. New data on the structure of the Cape Kamchatskiy, Eastern Kamchatka. *Transactions USSR Academy of Science, Earth Science Section*. **285**, 4, 89-92. (in Russian).
- ZINKEVICH V.P., KONSTANTINOVSKAIA E.A., TSUKANOV N.V., et al. Pushcharovskiy Yu.M. (ed.) 1993. *Accretionary tectonics of the Eastern Kamchatka*, Nauka, Moscow, 272 p. (in Russian).

- ZINKEVICH V.P. & TSUKANOV N.V., 1993. Accretionary tectonics of Kamchatka. *International Geological Review* **35**, 953-973.
- ZLOBIN S.K. & ZAKARIADZE G.S. 1985. Geochemistry of the island arc plutonic complexes and their paleoanalogies. *Geochemistry* **11**, 1567-1577. (in Russian).
- ZLOBIN S.K. & ZAKARIADZE G.S. 1993. Magmatism, Metamorphism, and Geodynamics of Active plate Margins Exemplified by the Mesozoic Tethys. 413-433. Nauka, Moscow. (in Russian).
- ZULEGER E. and ERZINGER J. 1988. Determinations of the REE and Y in silicate materials with ICP-AES. *Fresenius Z. Analytic. Chemistry*. **332**, 140-143.

Table 1: ultramafic rocks, gabbroic rocks, and plagiogranites from southern Kamchatka Mys Peninsula

Locality	Mt. Soldatskaya Massif					Olenegorsk Pluton				
Rock	Spinel peridotite					Plag. peridotite		Ultramafic enclaves		
Sample	9846/1	9849/1	9849/3	9851/1	9852/1	9814/4	9814/10	0225/2	0230/1	0243/1
SiO ₂	40.4	37.5	43.8	43.7	38.9	40.7	40.4	40.5	37.2	41.0
TiO ₂	0.005	0.008	0.006	0.005	0.005	0.07	0.07	0.02	0.02	0.08
Al ₂ O ₃	0.4	0.5	0.6	0.6	0.1	10.0	8.2	0.60	0.60	6.6
Fe ₂ O ₃	3.17	4.45	1.50	1.37	2.97	5.22	4.61	4.83	5.97	5.93
FeO	4.61	3.08	6.45	6.73	5.20	3.66	4.35	4.64	2.58	3.8
MnO	0.13	0.12	0.14	0.14	0.14	0.14	0.15	0.11	0.13	0.11
MgO	41.9	39.1	43.8	44.2	46.6	24.0	25.9	37.9	38.5	27.1
CaO	0.61	0.85	0.78	0.84	0.10	7.49	7.36	0.48	0.14	6.51
Na ₂ O	b.l.	b.l.	b.l.	b.l.	b.l.	0.24	0.09	0.01	b.l.	0.10
K ₂ O	b.l.	b.l.	b.l.	b.l.	b.l.	0.02	b.l.	b.l.	b.l.	b.l.
P ₂ O ₅	0.01	0.01	0.01	0.01	0.01	0.01	0.01	0.02	0.02	0.02
H ₂ O ⁺	7.53	13.1	0.86	0.45	4.17	8.06	8.22	10.9	14.6	8.92
CO ₂	0.37	0.53	0.16	0.10	0.34	0.23	0.23	0.25	0.38	0.17
Total	99.13	99.25	98.12	98.19	98.53	100.05	99.62	100.29	100.17	100.27
Mg#	90.9	90.8	90.9	90.8	91.4	83.6	84.4	88.3	89.7	84.1
Sr	1.3	1.7	1.8	1.5	1.8	41	33	10	4	9
Zr	3	4	4	4	2	n.d.	n.d.	14	17	16
Sc	6.5	7.7	10	9.3	3.5	16	19			
V	27	24	31	25	7	43	55	39	34	71
Cr	2649	2962	2972	2492	2909	740	1134	2672	2720	1559
Ni	2191	2206	2189	2217	2396	725	765	2040	2539	1116
Zn	43	48	45	45	44	54	54	43	46	30
Y	0.06	0.099	0.069	0.070	0.05	1.8	2.1	0.69	0.53	2.05
La	0.03	0.062	0.016	0.016	0.07	0.1	0.41	0.14	0.09	0.11
Ce	0.12	0.136	0.039	0.038	0.13	0.32	0.90	0.57	0.31	0.39
Pr	0.01	0.018	0.006	0.005	0.01	b.l.	0.13	0.04	0.04	0.06
Nd	0.03	0.071	0.025	0.023	0.04	0.35	0.50	0.18	0.20	0.33
Sm	0.1	b.l.	b.l.	b.l.	b.l.	0.15	0.19	0.05	0.07	0.16
Eu	b.l.	0.006	0.003	0.002	0.002	0.1	0.10	0.02	0.02	0.08
Gd	0.01	0.017	0.009	0.007	0.008	0.02	0.23	0.07	0.09	0.28
Tb	b.l.	0.003	0.002	0.001	0.001	b.l.	b.l.	0.01	0.01	0.05
Dy	0.01	0.017	0.011	0.009	0.009	0.3	0.35	0.10	0.10	0.37
Ho	b.l.	0.004	0.003	0.003	0.002	0.07	0.08	0.03	0.02	0.08
Er	0.01	0.013	0.010	0.011	0.006	0.19	0.25	0.09	0.07	0.25
Tm	b.l.	0.003	0.002	0.003	0.001	b.l.	b.l.	0.015	0.01	0.04
Yb	0.02	0.023	0.021	0.023	0.009	0.21	0.24	0.12	0.08	0.25
Lu	b.l.	0.005	0.005	0.005	0.002	0.04	0.04	0.02	0.01	0.04

Tab. 1 Continued

Locality	Olenegorsk Pluton						Olkhovaya Gabbro Block		
Rock	Gabbroic rocks						Gabbroic rocks		
Sample	9803/3	9803/4	9806/1	9831/1	9835/1	9837/1	9863/1	9863/2	9864/1
SiO ₂	47.4	50.7	48.9	46.3	46.6	46.8	53.7	42.8	47.0
TiO ₂	0.38	0.37	0.29	0.17	0.17	0.17	0.51	0.73	0.20
Al ₂ O ₃	18.9	15.0	15.7	20.2	19.3	18.9	13.3	16.1	17.0
Fe ₂ O ₃	2.46	2.26	1.82	1.63	2.58	2.66	2.17	7.64	2.80
FeO	4.50	5.17	3.51	2.46	2.66	2.69	5.20	8.79	4.83
MnO	0.12	0.16	0.11	0.08	0.09	0.08	0.17	0.19	0.16
MgO	8.97	10.0	10.4	9.85	10.3	9.76	9.43	7.59	9.05
CaO	12.0	12.0	14.2	12.6	13.4	13.8	8.60	12.4	15.2
Na ₂ O	2.21	2.02	1.67	1.76	1.2	1.57	3.48	0.69	0.61
K ₂ O	0.01		0.02	0.04	0.02	0.01	0.43	0.03	0.24
P ₂ O ₅	0.02	0.01	0.01	0.01	0.01	0.02	0.05	0.01	0.01
H ₂ O ⁺	2.70	1.92	2.74	4.11	2.71	2.65	2.25	2.48	2.46
CO ₂	0.07	0.07	0.13	0.14	0.15	0.11	0.06	0.08	0.11
Total	99.72	99.60	99.58	99.40	99.34	99.27	99.33	99.58	99.62
Mg#	70.4	71.3	78.3	81.7	78.6	77.4	70.1	46.3	68.7
Rb		2.0	0.95	0.33	0.88		3.9	0.47	3.6
Ba							30	10	13
Sr	114	96	89	132	95	104	200	149	162
Zr	21	12	10	60		8	46		5
Sc	22	40	42	19	24	26	41	53	59
V	115	182	165	66	83	93	200	783	205
Cr	215	309	1104	768	920	671	395	16	120
Ni	195	97	178	258	252	275	128	52	77
Zn	49	47	40	32	43	54	65	65	63
Y	8.7	9.5	9.0	14	4.5	4.9	13	4.2	5.6
La	1.1	0.80	0.35	2.2	0.68	0.74	2.0	0.29	0.47
Ce	2.5	1.7	1.0	6.7	1.5	1.9	5.4	0.74	0.86
Pr	0.46	0.28	0.30	1.2	0.24	0.30	1.0	0.27	0.22
Nd	2.6	1.9	1.5	5.2	1.1	1.4	4.5	0.82	1.2
Sm	0.82	0.74	0.70	1.5	0.46	0.54	1.4	0.22	0.53
Eu	0.50	0.47	0.40	0.61	0.31	0.33	0.53	0.19	0.23
Gd	1.2	1.1	1.1	1.8	0.62	0.68	1.9	0.56	0.80
Tb	0.18	0.20	0.20	0.36		0.11	0.34	0.17	n.d.
Dy	1.6	1.7	1.6	2.4	0.81	0.91	2.3	0.78	1.1
Ho	0.30	0.33	0.34	0.51	0.18	0.19	0.49	0.18	0.22
Er	1.1	1.2	1.1	1.6	0.49	0.58	1.6	0.41	0.84
Tm	0.16	0.17	0.17	0.25		0.10	0.24	0.12	0.15
Yb	0.88	1.1	0.93	1.6	0.48	0.53	1.4	0.53	0.66
Lu	0.15	0.17	0.15	0.27	0.07	0.09	0.22	0.09	0.10

Tab. 1 Continued

Locality	Olkhovaya Gabbro Block										
Rock	Gabbroic rocks			Anorth. Plagiogranite							
Sample	0260/2	0262/1	0269/1	9842/6	9863/5	9865/1	M11/1	M11/6	M12/1	M12/3	M16
SiO ₂	49.3	47.9	43.4	44.9	68.5	72.3	77.0	71.9	74.2	74.7	75.7
TiO ₂	0.16	0.37	0.91	0.09	0.53	0.30	0.33	0.41	0.16	0.30	0.40
Al ₂ O ₃	16.5	15.7	15.9	29.0	13.0	13.4	12.1	12.7	12.4	11.3	12.4
Fe ₂ O ₃	1.08	2.84	7.14	1.58	3.32	2.09	1.28	3.28	1.81	1.52	1.76
FeO	4.86	7.45	9.36		4.15	1.12	0.86	1.65	1.29	0.79	0.86
MnO	0.14	0.20	0.20	0.02	0.18	0.07	0.04	0.07	0.06	0.04	0.03
MgO	9.23	8.61	7.19	4.30	0.74	0.73	0.65	0.73	0.74	0.88	0.89
CaO	14.7	10.6	10.8	15.4	4.32	3.13	2.14	2.92	2.97	3.92	1.57
Na ₂ O	1.43	2.42	1.69	1.37	3.47	4.38	0.92	0.38	3.90	0.15	0.31
K ₂ O	0.13	0.29	0.15	0.03	0.15	0.40	3.80	4.20	0.29	4.09	5.12
P ₂ O ₅	0.02	0.04	0.03	0.01	0.11	0.06	0.03	0.07	0.07	0.04	0.06
H ₂ O ⁺	1.89	3.17	2.16	2.54	0.78	1.33	LOI=	LOI=	1.06	LOI=	LOI=
CO ₂	0.11	0.08	0.07	0.16	0.04	0.06	0.90	1.35	0.06	2.17	0.90
Total	99.56	99.67	98.98	99.40	99.30	99.38	100.08	99.61	98.96	99.92	100.04
Mg#	73.9	60.7	44.9	84.3	15.6	30.2	36.6	24.3	31.2	42.7	39.4
Rb	b.l.	b.l.	b.l.	0.40	0.98	5	11	2	1.6	1	2
Ba	13	50	16		35	68	279	74	37	16	39
Th					0.09	0.32	1.55	0.24	0.20	0.36	0.64
U					0.04	0.21	0.61	0.17	0.08	0.24	0.23
Nb					1.6	1.0	1.54	0.60	0.6	0.84	0.94
Ta					0.05	0.06	0.14	0.05	0.02	0.07	0.09
Sr	117	116	107	144	168	165	156	232	215	116	144
Zr	19	20	20		57	86	72	14	71	27	45
Hf	b.l.	b.l.	b.l.	0.10	0.39	0.62	2.57	0.68	0.4	1.19	1.75
Sc	55	55	56	2.4	25	13	8	17	13	16	12
V	152	230	793	18	3	34	30	18	7	24	27
Cr	329	22	7	43	1	3	20	9	5	8	16
Ni	97	56	25	140	2	2	15	7	5	7	9
Zn	43	57	67	20	89	48			20		
Y	5.0	7.7	5.9	1.8	25	20	17	23	20	30	14
La	0.45	0.70	0.55	0.36	2.8	4.1	5.86	2.43	4.2	4.67	5.25
Ce	1.1	1.8	1.3	1.2	8.1	10	12.2	6.07	10	10.7	10.2
Pr	0.20	0.33	0.23	0.20	1.6	1.7	1.59	1.04	1.7	1.64	1.39
Nd	1.1	1.8	1.2	0.90	8.6	7.8	6.73	5.95	7.8	8.19	6.13
Sm	0.42	0.70	0.51	0.22	2.8	2.4	1.68	2.13	2.4	2.49	1.58
Eu	0.19	0.29	0.27	0.22	1.4	0.69	0.61	0.90	0.69	0.89	0.47
Gd	0.65	1.0	0.77	0.31	3.9	2.8	2.07	3.00	2.8	3.57	1.93
Tb		0.22			0.70	0.47	0.36	0.53	0.47	0.67	0.32
Dy	0.83	1.3	0.98	0.32	4.9	3.3	2.48	3.68	3.3	4.65	2.21
Ho	0.18	0.28	0.22		1.0	0.66	0.57	0.83	0.66	1.08	0.49
Er	0.57	0.91	0.69	0.15	3.1	2.3	1.75	2.40	2.3	3.22	1.42
Tm				0.03	0.46	0.34	0.29	0.36	0.34	0.49	0.22
Yb	0.56	0.88	0.67	0.16	2.7	2.4	2.01	2.34	2.4	3.08	1.42
Lu	0.09	0.14	0.10	0.03	0.41	0.38	0.33	0.35	0.38	0.48	0.22

Samples M11/1, M11/6, M12/3 and M16 were analyzed at the Analytical Center of the Geological Institute of the Russian Academy of Science, Moscow (major components) and at the Institute of Mineralogy and Geochemistry of Trace Elements (rare elements, analyst: D.Z. Zhuravlev).

Mg# = 100MgO/(MgO+FeO), FeO = FeO + 0.9Fe₂O₃

Location of the samples see in Fig. 1, Fig. 2 and Fig. 4

Tab.2: Volcanic and subvolcanic rocks from southern Kamchatka Mys Peninsula

Locality	Olenegorsk Massif			Kamensk Complex				Afrika Complex			
Rock	Dolerite, nMORB-type			Transitional basalt	nMORB-type basalt			nMORB-type basalt			
Sample	9801/3	9801/5	9829/1	9808/1	9808/2	9822/1	9838/2	9840/1	9857/3	9867/1	9867/2
SiO ₂	48.4	48.8	48.9	47.4	46.9	47.6	47.8	47.2	46.7	42.9	50.5
TiO ₂	1.22	1.28	1.43	1.67	1.58	1.25	1.45	1.45	1.50	1.99	1.37
Al ₂ O ₃	16.7	14.9	15.8	15.2	15.1	17.4	17.1	17.2	13.5	11.9	15.4
Fe ₂ O ₃	3.25	2.92	3.44	7.21	7.83	5.37	5.27	5.39	6.20	7.67	8.57
FeO	5.88	6.21	6.43	2.77	2.51	3.67	3.70	4.08	5.58	4.76	3.05
MnO	0.18	0.19	0.17	0.2	0.19	0.16	0.16	0.16	0.20	0.24	0.16
MgO	8.03	8.94	7.46	7.16	5.69	6.45	6.19	6.02	7.04	6.46	4.47
CaO	11.9	10.8	11.4	8.39	10.3	10.6	9.60	9.86	10.2	12.5	6.38
Na ₂ O	2.01	2.45	2.45	2.83	3.37	2.91	3.20	3.57	3.11	2.32	5.52
K ₂ O	0.05	0.26	0.04	2.02	1.42	0.68	1.32	0.71	0.97	1.41	0.04
P ₂ O ₅	0.11	0.11	0.10	0.21	0.23	0.15	0.15	0.16	0.12	0.13	0.16
H ₂ O ⁺	2.2	2.84	2.07	3.85	3.39	2.99	3.33	3.60	2.67	3.31	3.56
CO ₂	0.1	0.17	0.13	0.51	0.85	0.55	0.62	0.39	1.77	4.80	0.33
Total	100.03	99.87	99.82	99.42	99.36	99.78	99.89	99.79	99.56	100.39	99.51
Mg#	61.9	64.3	58.2	57.9	51.5	57.5	56.6	54.6	52.9	49.7	42.5
Rb	0.26	1.4	0.08	23	15	11	17	10	26	22	0.55
Cs	0.01	b.l.	b.l.	0.61	0.46	0.22	0.22	0.33	0.80	0.42	0.01
Ba	7	19	12	47	45	38	74	88	175	80	27
Th	0.08	0.13	0.06	0.52	0.48	0.17	0.18	0.18	0.11	0.13	0.27
U	0.04	0.05	0.01	0.22	0.19	0.12	0.08	0.10	0.11	0.28	0.14
Nb	1.5	2.7	1.2	8.0	7.0	2.9	2.5	2.6	1.3	2.0	1.5
Ta	0.14	0.20	0.10	0.46	0.43	0.21	0.18	0.18	0.11	0.13	0.11
Sr	100	123	113	119	131	162	240	154	179	80	71
Zr	74	73	84	113	105	86	109	108	77	117	62
Hf	1.9	1.4	1.2	3.2	3.0	2.3	2.7	2.8	2.2	3.0	1.8
Sc	36	43	36	40	38	35	37	33	45	41	32
V	273	274	304	312	309	260	261	264	349	375	407
Cr	471	356	260	242	237	454	339	336	240	117	8
Ni	128	92	95	125	98	147	101	98	58	54	18
Zn	103	59	70	97	83	81	83	83	108	134	100
Y	27	26	27	36	36	28	33	30	32	42	26
La	2.3	3.0	2.3	5.7	6.0	3.3	3.9	4.1	2.6	3.4	4.6
Ce	8.0	8.6	8.0	15	15	10	13	14	9.2	13	12
Pr	1.5	1.5	1.5	2.6	2.6	1.8	2.2	2.2	1.8	2.1	2.1
Nd	7.7	8.3	8.0	13	13	9.1	11	11	8.6	12	10
Sm	2.8	2.9	2.9	4.0	4.0	3.0	3.9	3.6	3.2	4.0	3.2
Eu	1.0	1.1	1.1	1.5	1.4	1.1	1.4	1.3	1.2	1.4	1.2
Gd	4.0	4.0	4.0	5.4	5.3	4.3	5.1	4.7	4.5	5.7	4.0
Tb	0.7	0.70	0.70	1.0	0.95	0.76	0.90	0.83	0.89	1.1	0.74
Dy	4.9	5.0	5.0	6.6	6.4	5.4	6.1	5.7	5.8	7.5	4.7
Ho	1.0	0.95	1.1	1.4	1.4	1.1	1.2	1.1	1.2	1.5	0.98
Er	3.3	3.2	3.5	4.2	4.1	3.3	3.9	3.7	3.9	4.8	3.0
Tm	0.48	0.47	0.49	0.62	0.62	0.51	0.60	0.51	0.58	0.73	0.43
Yb	3.0	2.9	3.1	3.9	3.8	3.1	3.6	3.2	3.7	4.5	2.8
Lu	0.45	0.44	0.47	0.57	0.57	0.46	0.55	0.50	0.56	0.71	0.42

Location of the samples see in Fig. 2.

Tab.3: Ophiolite members, Kronotsky Peninsula

Locality	Kronotsky melange							
Rock	Serpentinites							Pyroxenite
Sample	99105/2	99133/1	99135	869	882	882/18	1140/2	99107
SiO ₂	38.5	38.7	38.5	36.0	36.8	38.4	37.4	43.6
TiO ₂	0.02	0.02	0.02	0.01	0.02	0.02	0.02	0.10
Al ₂ O ₃	1.2	1.3	1.3	0.70	0.90	0.90	1.2	2.0
Fe ₂ O ₃	6.24	5.96	5.39	6.42	5.95	4.61	5.48	7.49
FeO	2.11	2.64	3.1	2.17	2.44	3.78	2.85	10.5
MnO	0.12	0.13	0.12	0.13	0.12	0.13	0.12	0.32
MgO	37.7	38	38	38.6	38.2	38.0	37.8	25.7
CaO	1.45	0.26	1.45	0.29	0.87	0.10	0.90	2.67
Na ₂ O	0.09	0.1	0.1	b.l.	0.01	b.l.	b.l.	0.19
K ₂ O	b.l.	0.02	0.2	b.l.	b.l.	b.l.	b.l.	0.01
P ₂ O ₅	0.02	0.02	0.02	0.02	0.02	0.02	0.02	0.02
H ₂ O ⁺	11.8	12.9	11.4	14.9	14.3	13.9	13.7	7.09
CO ₂	0.40	0.42	0.35	0.77	0.65	0.32	0.67	0.14
Total	99.72	99.83	99.58	100.07	100.32	100.21	100.20	99.87
Mg#	91.4	89.5	89.6	89.6	89.7	89.5	89.7	72.4
Sr	2.5	4	3.5	5	7	3	3	2.5
Zr	3	3	5	14	12	12	13	4
Sc	3	4.1						64
V	42	50	44	26	35	39	45	258
Cr	2692	2816	2670	2134	1960	2609	3053	1088
Ni	2366	2377	2340	2622	2510	2473	2423	917
Zn	43	46	44	40	48	42	45	101
Y	0.292	0.420	0.384	0.20	0.30	0.23	0.26	1.53
La	0.027	0.121	0.051	0.09	0.07	0.14	0.08	0.138
Ce	0.054	0.204	0.105	0.27	0.23	0.34	0.36	0.307
Pr	0.005	0.020	0.013	0.02	0.02	0.02	0.02	0.045
Nd	0.020	0.068	0.055	0.09	0.10	0.08	0.07	0.212
Sm	0.006	0.015	0.016	0.02	0.03	0.01	0.02	0.067
Eu	0.003	0.005	0.006		0.01		0.01	0.022
Gd	0.014	0.024	0.025	0.02	0.04	0.02	0.02	0.103
Tb	0.004	0.005	0.006		0.01			0.024
Dy	0.040	0.053	0.055	0.03	0.05	0.03	0.04	0.220
Ho	0.011	0.014	0.015	0.01	0.01	0.01	0.01	0.063
Er	0.043	0.054	0.056	0.03	0.04	0.03	0.04	0.254
Tm	0.008	0.010	0.010	0.01	0.01	0.01	0.01	0.049
Yb	0.063	0.078	0.081	0.06	0.06	0.05	0.06	0.427
Lu	0.012	0.014	0.015	0.01	0.01	0.01	0.01	0.078

Tab. 3: Continued

Locality	Kronotsky melange										
Rock	Gabbroic rocks			Dolerites, BABB-type			MORB-type basalts				
Sample	99128/1	99128/2	99130/1	99103/3	99120/2	99129	99130/2	881	881/1	1407	1408/13
SiO ₂	52.6	53.9	49.9	48.8	51.0	51.7	52.1	46.7	45.6	46.9	45.1
TiO ₂	0.38	0.52	0.29	0.79	0.95	1.22	1.04	2.5	1.87	1.43	1.48
Al ₂ O ₃	14.1	15.9	12.9	16.7	14.6	14.5	15.0	14.8	15.2	15.0	14.7
Fe ₂ O ₃	1.21	2.54	1.03	4.54	7.42	2.59	2.61	6.35	5.29	6.05	5.50
FeO	6.32	5.60	7.12	5.93	5.5	7.94	8.69	7.23	6.11	4.67	5.33
MnO	0.15	0.13	0.16	0.18	0.23	0.19	0.20	0.22	0.21	0.15	0.19
MgO	8.94	5.93	11.1	5.0	5.37	6.83	3.88	6.22	7.23	6.89	7.17
CaO	11.9	11.5	12.0	9.92	9.18	9.25	9.75	11.2	10.9	8.27	10.3
Na ₂ O	1.00	0.39	1.18	3.25	2.80	2.39	2.97	2.65	2.52	4.47	3.00
K ₂ O	0.41	0.23	0.28	1.22	0.58	0.53	0.76			0.41	0.82
P ₂ O ₅	0.07	0.06	0.05	0.10	0.12	0.11	0.15	0.24	0.16	0.13	0.14
H ₂ O ⁺	2.64	2.82	2.80	2.61	2.05	1.70	2.43	1.25	1.54	2.95	2.21
H ₂ O ⁻								1.33	2.29	2.07	2.22
CO ₂	0.21	0.13	0.20	0.15	0.11	0.05	0.21		0.14	0.43	1.08
Total	99.91	99.56	99.05	99.19	99.91	99.00	99.79	100.	99.06	99.8	99.24
								69		2	
Mg#	59.9	57.3	71.0	48.9	44.0	54.2	38.5	46.1	54.2	54.8	55.4
Rb	1.9	1.7	1.0	11.0	5.8	2.5	4.4	0.99	1.81	8.78	10.8
Cs	0.06	0.02	0.03	0.13	0.10	0.03	0.02		0.04	0.09	0.16
Ba	22	14	21	124	86	33	79	6.75	16.6	18	101
Th	0.29	0.21	0.34	0.13	0.14	0.12	0.28	0.26	0.14	0.13	0.14
U	0.15	0.13	0.12	0.10	0.08	0.06	0.11	0.19	0.09	0.14	0.29
Nb	0.49	0.46	0.36	1.0	0.31	1.1	1.1	4.48	2.36	1.91	1.87
Ta	0.09	0.07	0.04	0.05	0.02	0.10	0.09	0.30	0.17	0.14	0.12
Sr	137	161	223	221	162	130	185	123	129	91.1	291
Zr	34	35	20	37	53	60	58	190	117	86.1	96.8
Hf			0.56	1.0		1.1		4.87	3.22	2.37	2.60
Sc	40	36	48	43	50	39	32				
V	235	265	249	393	462	334	294				
Cr	270	27	546	43	33	166					
Ni	91	36	142	24	21	72	11				
Zn	42	83	52	63	83	62	60				
Y	10	12	7.0	17	21	23	24	54.1	37.4	28.7	31.8
La	2.7	2.0	1.7	2.2	2.5	2.7	4.1	5.73	3.47	3.20	2.93
Ce	6.4	4.8	3.7	6.2	7.2	8.2	11	18.7	11.5	9.62	9.83
Pr	1.0	0.81	0.61	1.2	1.2	1.5	1.9	3.24	2.06	1.65	1.74
Nd	4.4	3.9	2.8	5.7	7.0	7.7	8.7	17.8	11.5	9.12	9.82
Sm	1.3	1.3	0.89	1.9	2.3	2.5	2.6	6.07	4.16	3.18	3.49
Eu	0.36	0.49	0.33	0.70	0.86	0.95	0.98	2.01	1.47	1.17	1.22
Gd	1.6	1.8	1.1	2.4	3.1	3.4	3.3	8.48	5.93	4.54	4.79
Tb	0.25	0.31	0.17	0.40	0.55	0.62	0.60	1.48	1.00	0.75	0.84
Dy	1.7	2.1	1.2	3.1	3.7	4.2	3.9	9.75	6.94	5.15	5.70
Ho	0.36	0.46	0.26	0.65	0.78	0.88	0.81	2.08	1.47	1.09	1.19
Er	1.1	1.4	0.80	2.1	2.5	2.8	2.7	6.22	4.37	3.33	3.60
Tm	0.19	0.24	0.14	0.32	0.37	0.41	0.39	0.90	0.61	0.45	0.52
Yb	1.2	1.5	0.87	1.9	2.4	2.6	2.5	5.96	4.00	3.06	3.44
Lu	0.19	0.23	0.13	0.29	0.37	0.40	0.44	0.87	0.59	0.46	0.50

The major components of samples 881 to 1408-13 were analyzed in the Kamchatskaya Searching Mapping Expedition.

Location of the number samples see in Fig. 1

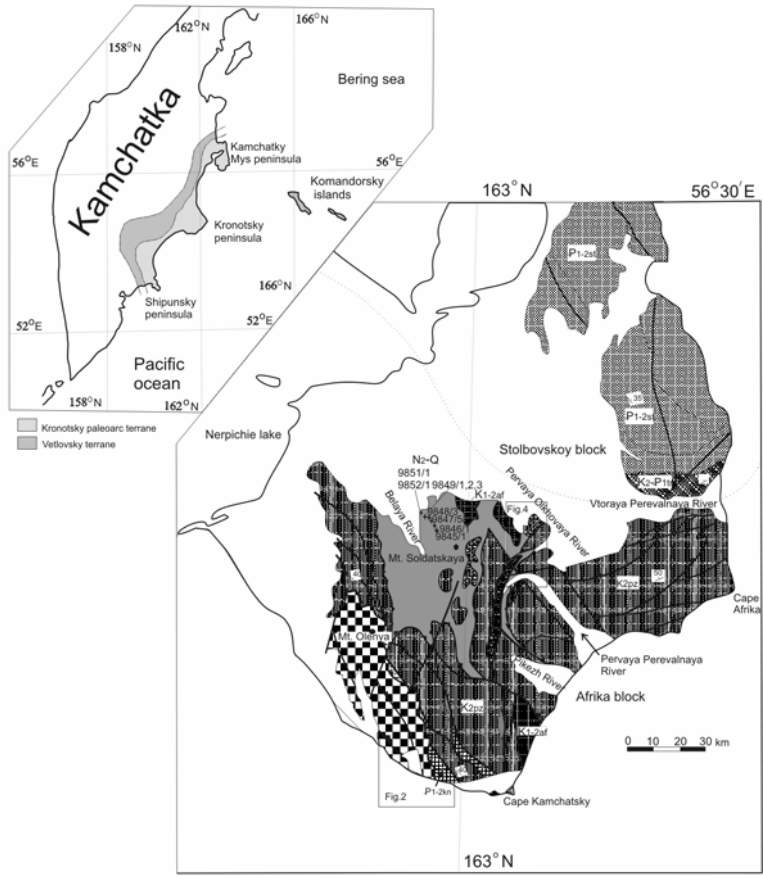


Fig 1a

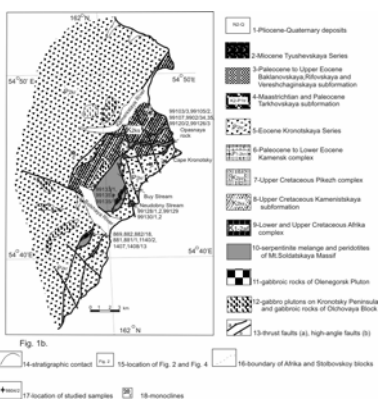


Fig. 1b.

14-stratigraphic contact 15-location of Fig. 2 and Fig. 4 16-boundary of Afrika and Stolbovskiy blocks
 17-location of studied samples 18-monoclines

Fig. 2. Tsukanov et al.

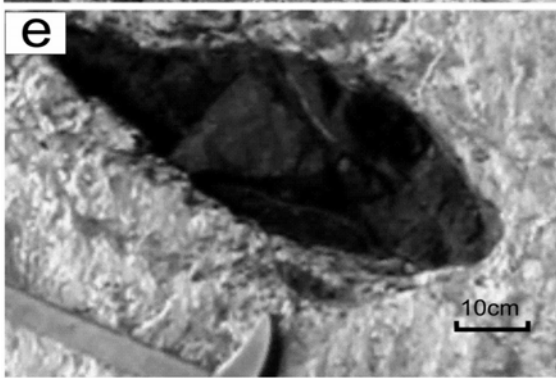
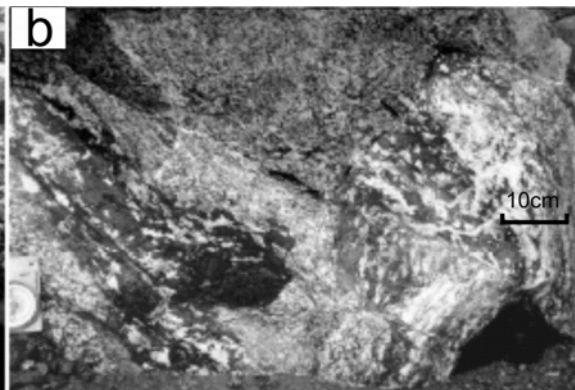
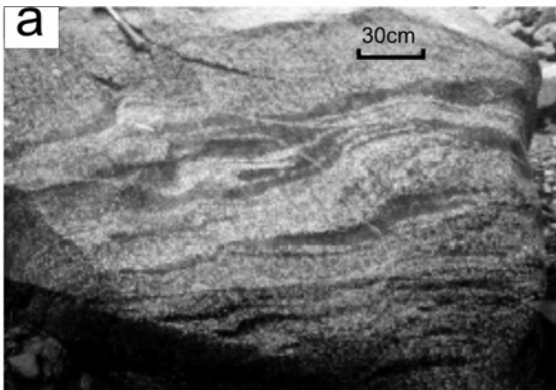
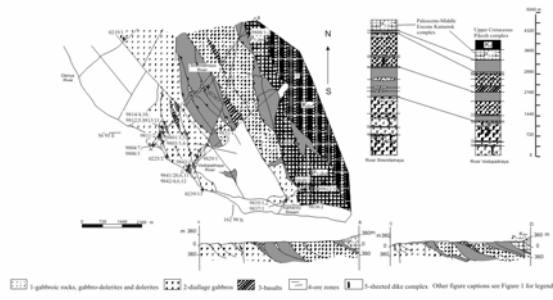


Fig. 4. Tsukanov et al.

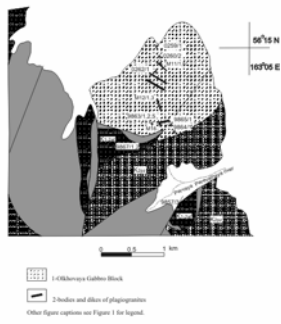
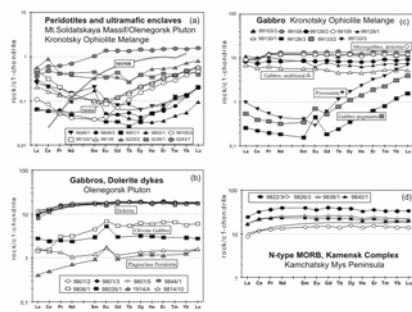


Fig. 5. Tsukanov et al.



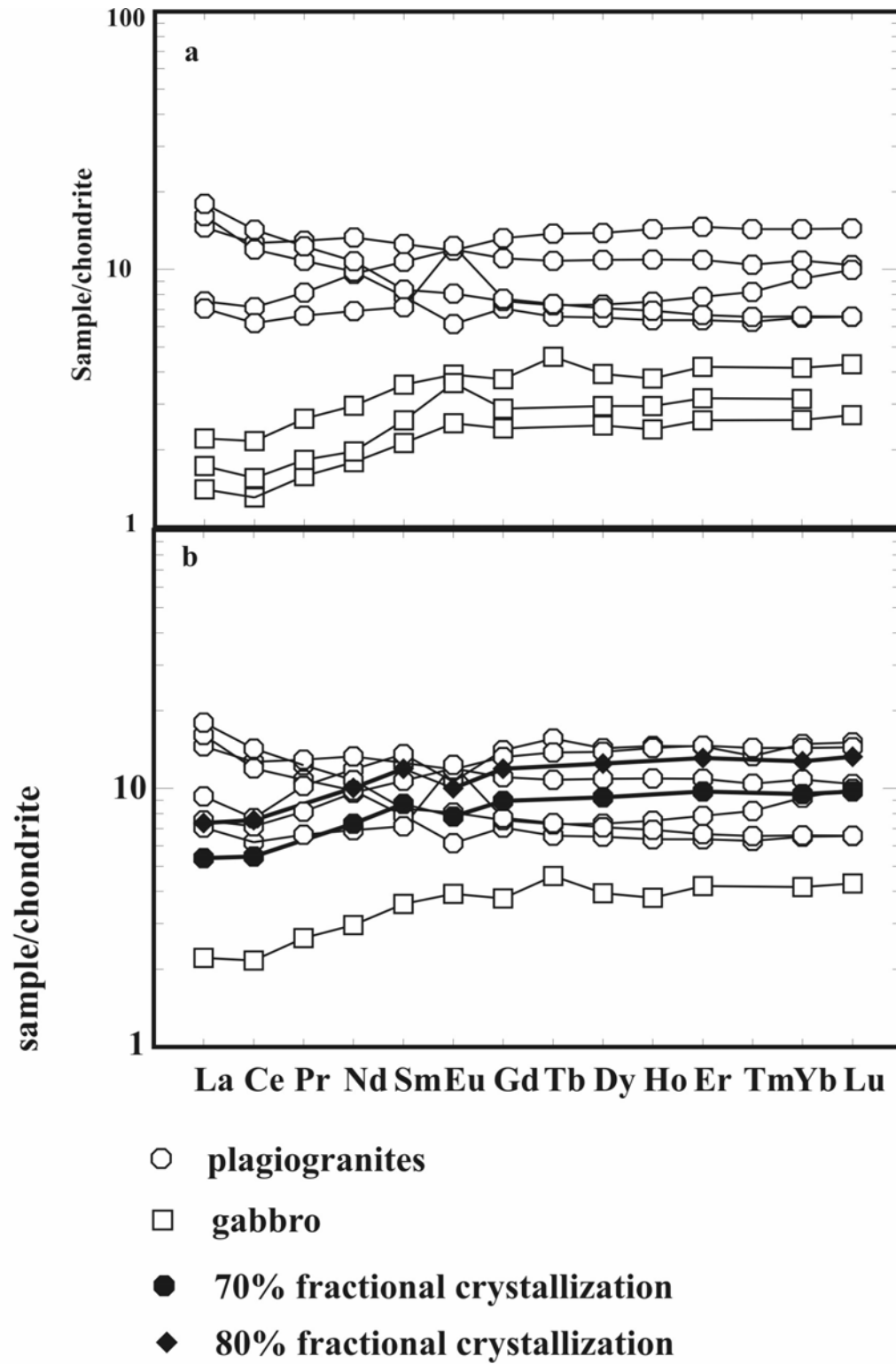


Fig. 6. Tsukanov et al.

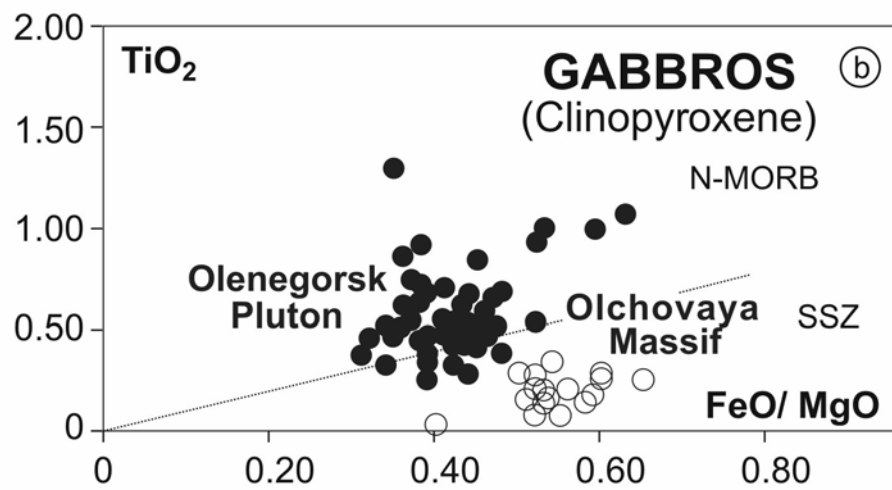
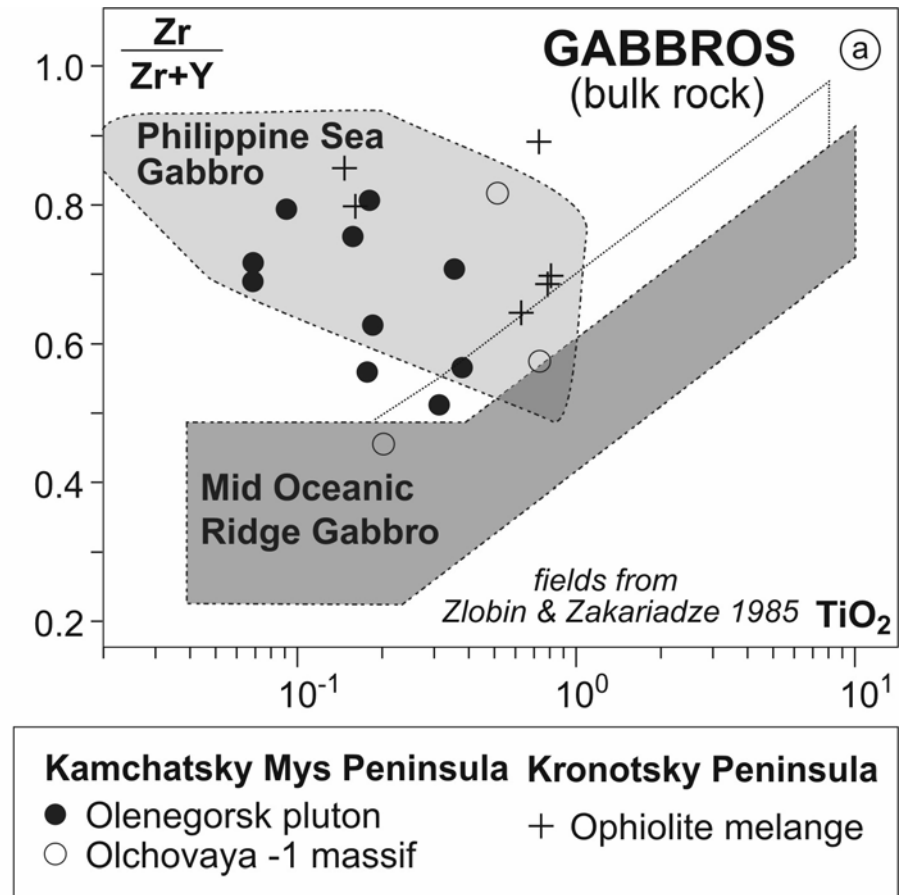


Fig. 7. Tsukanov et al.

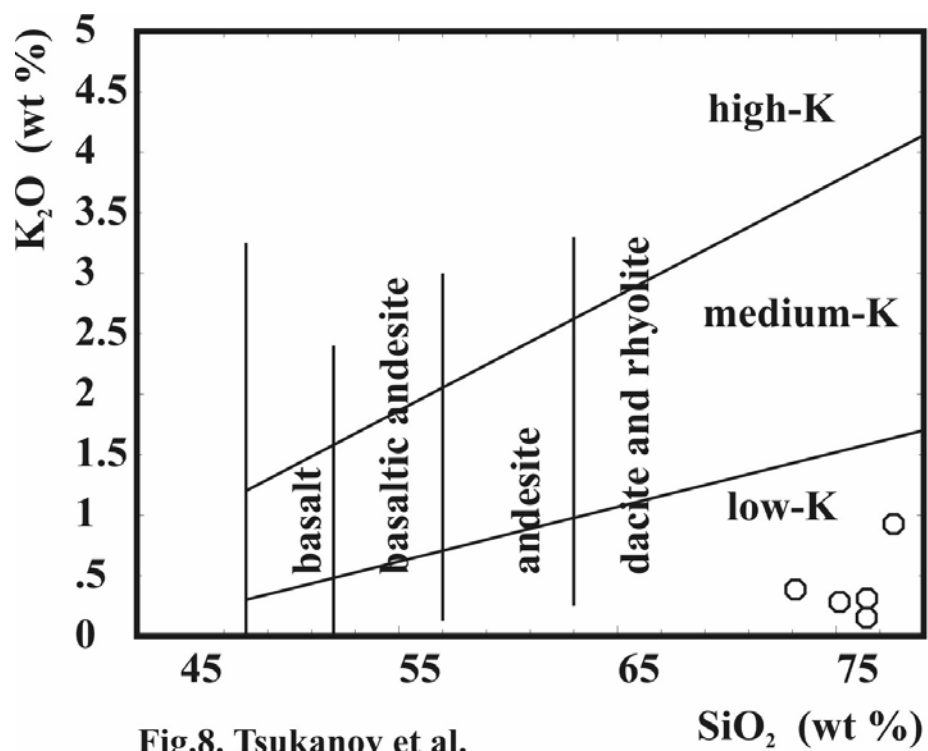


Fig.8. Tsukanov et al.

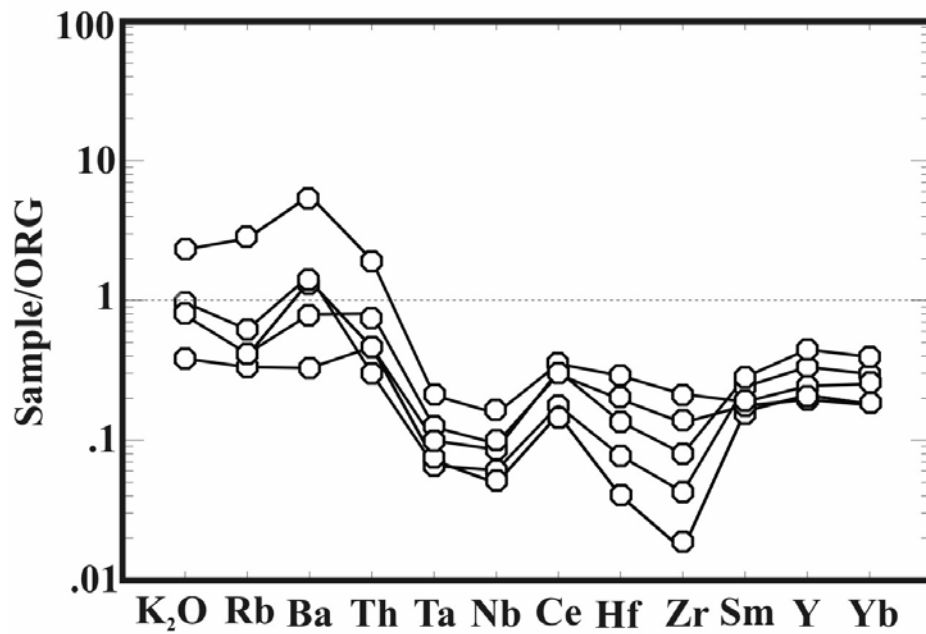
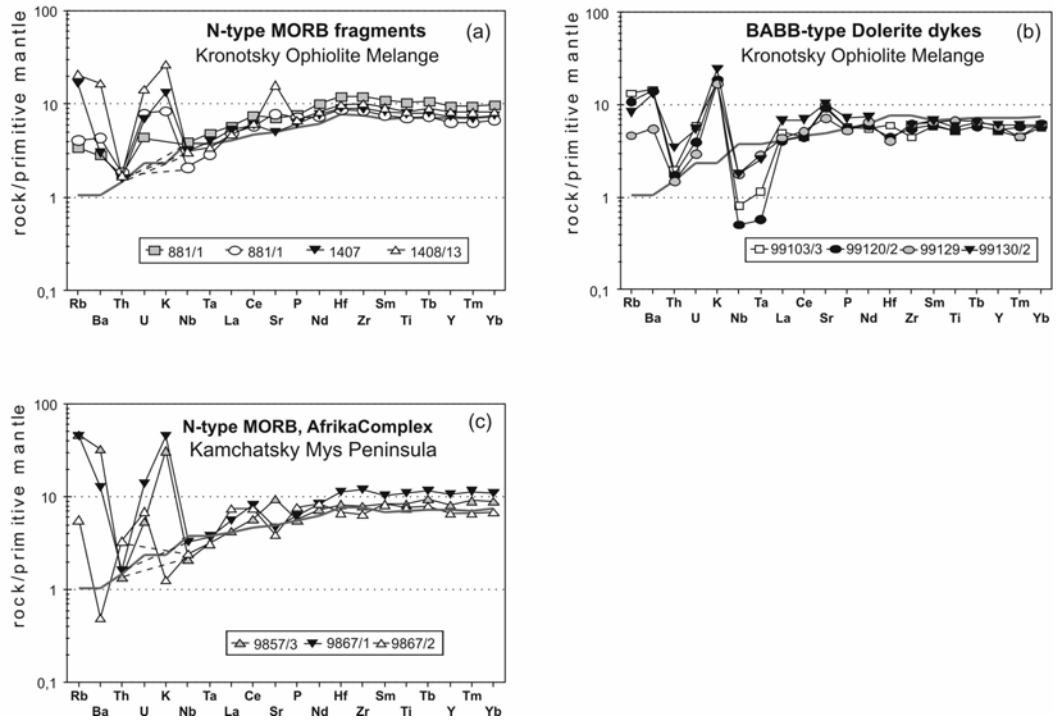


Fig. 9. Tsukanov et al.

Fig. 10. Tsukanov et al.



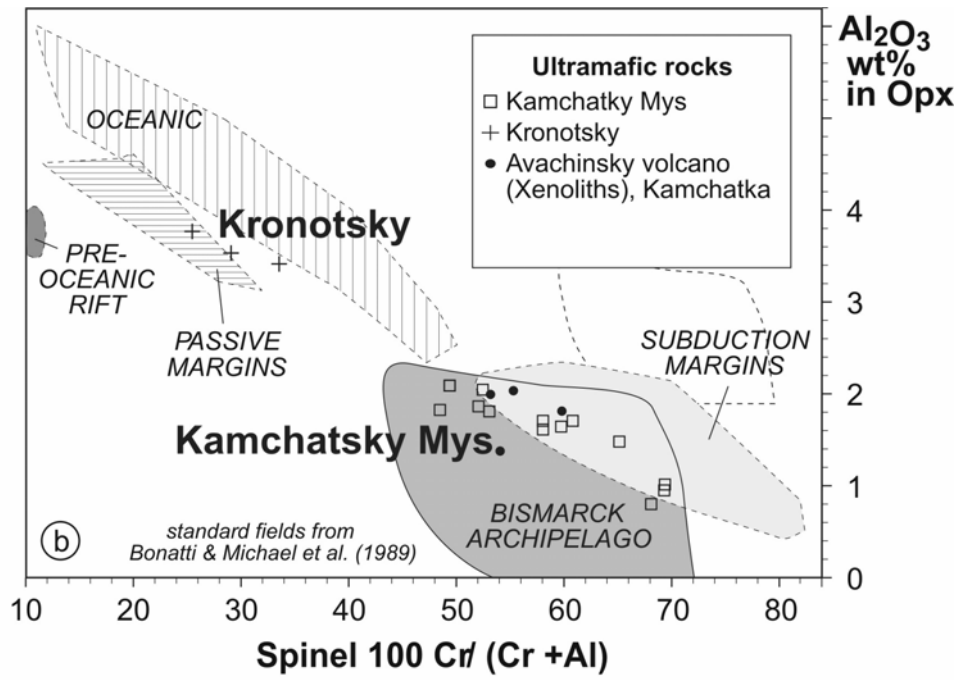


Fig. 11. Tsukanov et al.

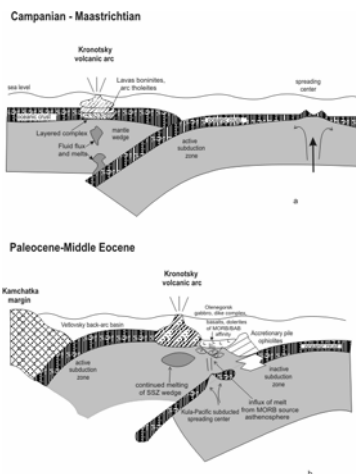


Fig. 12. Tsukanov et al.

Figure captions

Fig. 1a,b. Geological map of Kamchatsky Mys (a) and Kronotsky (b) peninsulas (modified from Zinkevich et al. 1985, Raznitsyn et al. 1985)

Fig. 2 Geological map of Olenegorsk Pluton

Fig. 3. Xenoliths and textures in gabbros of the Olenegorsk Pluton. (a) Rhythmic texture in gabbros. (b) Troctolite and peridotite xenoliths in olivine gabbro. (c) to (e) Xenoliths of serpentinite in gabbro. (f) Xenoliths of fine-grained gabbro in plagiogranites.

Fig. 4. Geological map of Pervaya Olkhovaya and Pervaya Perevalnaya Rivers (Kamchatsky Mys Peninsula), based on the works of Boyarinova, 2000 and Zinkevich et al. 1985.

Fig. 5. Comparison of the chondrite-normalized REE patterns of ophiolitic rocks from Kamchatsky Mys and Kronotsky peninsulas. Normalizing values according to Evensen et al. (1978). (a) The ultramafic rocks form three distinct groups, based on the distribution of the heavy REE: 9849/1 to 9852/1 from the Mt. Soldatskaya Massif; 99105/2 to 99135 from the Kronotsky Melange; 0225/2 to 0243/1 are enclaves from the Olenegorsk Pluton. MOMR: mid-oceanic ridge mantle residues of the internal Ligurides (Rampone et al. 1996); SSZO: supra-subduction zone ophiolitic peridotite (Kay & Senechal 1976). (b) The gabbroic components of the Olenegorsk Pluton show distinct positive Eu anomalies. Samples 9801/2 to 9844/1 are cross-cutting (sheeted dyke) dolerites congruent with N-type MORB averages according to Sun and McDonough (1989). (c) The gabbroic fragments of the Kronotsky Ophiolite Melange. Samples 99103/3, 99128/1, and 99130/1: microgabbros, doleritic; 99108, 99109, and 99128/2: gabbros, uralitized. The gabbro-pegmatites display positive Eu anomalies like the Olenegorsk gabbros. (d) N-MORB from Southern Kamchatsky Mys with weak negative Eu anomalies.

Fig. 6. a) Normalized REE patterns of the gabbros and plagiogranite from - Pervaya Olkhovaya River. b) Calculated acid liquids from 70% and 80% fractional

crystallization of parental gabbroic liquid. Sample 0262/1 gabbro is considered to approximate the initial composition that underwent fractionation. The equation of Rayleigh fractionation law $C_L = C_0 * F^{(D-1)}$ is used. Distribution coefficients are taken from (Rollinson 1993). Normalizing values from (Sun & McDonough, 1989).

Fig. 7. Zr/Zr+Y vs TiO₂ (a), TiO₂ vs FeO/MgO (Zlobin and Zakariadze, 1985) (b) diagrams for clinopyroxenes from gabbroic rocks of Kamchatsky Mys and Kronotsky peninsulas ophiolite complexes. On (b) The line separates dashed fields of supra-subduction zone (low) and oceanic tholeiite (upper) gabbroic rocks.

Fig. 8. SiO₂ vs K₂O diagram for plagiogranites from Kamchatsky Mys ophiolite complex

Fig. 9. ORG-normalized patterns for plagiogranites from Kamchatsky Mys ophiolite complex. Normalizing values from Pearce et al. (1984)

Fig. 10. Extended trace element distribution patterns of tholeiitic volcanic and dyke rock fragments from the Eastern Kronotsky and Southern Kamchatsky Mys Peninsulas, primitive mantle normalized according to Hofmann (1988). Each diagram includes the N-type MORB averages according to Sun and McDonough (1989). The hatched line sections between Th and Nb in diagrams (a) and (c) excludes the mobile elements U and K. Those generalized curves point to the similarity with the N-type MORB averages. The patterns of N-type MORBs from the Southern Kamchatsky Mys Peninsula (c) and of the Kronotsky Melange basalt fragments (a) are nearly congruent. However, the BABB-type dolerite dyke fragments from the Kronotsky Ophiolite Melange (b) display strong Nb-Ta anomalies.

Fig. 11. Al₂O_{3(sp)} vs 100Cr/(Cr+Al)_(opx) plot of spinel peridotites with fields after Bonatti and Michael (1989).

Fig. 12. Schematic illustration of the evolution Kronotsky paleoarc in Campanian – Maastrichtian (a) and Paleocene - Middle Eocene (b) time (no scale).